Morphology and performance of the “trap-jaw” cheliceral strikes in spiders (Araneae, Mecysmaucheniidae)

Author: Hannah M. Wood
Department Entomology, National Museum of Natural History, Smithsonian Institution, Washington, DC 20013 USA.

Corresponding author’s email: woodh@si.edu

Summary statement: Morphological shifts are documented for the fastest known arachnid movement, the cheliceral strike in mecysmaucheniid spiders. The energy-storage mechanism used to achieve these ultra-fast speeds is described.

ABSTRACT

Mecysmaucheniidae spiders have evolved ultra-fast cheliceral strikes four times independently. The mechanism for producing these high-speed strikes is likely due to a latch/spring system that allows for stored energy to be rapidly released. This study examines two different sister-lineages: *Zearchaea* has ultra-fast cheliceral strikes and *Aotearoa*, based on external morphology, is hypothesized to have slower strikes. Using high-speed videography, I gather kinematic data on each taxon and test the hypothesis that external morphology predicts cheliceral strike performance. Then, using histology and data from µ-Computed-Technology scanning I ask whether internal muscle morphologies also correspond to performance differences. Results from high-speed video analysis reveal that *Zearchaea* sp. achieves peak angular velocities of 25.0 ± 4.8 x 10^3 rad s^{-1} (mean ± standard deviation) in durations of 0.0843 ± 0.017 ms. The fastest recorded strike had a peak angular and linear velocity of 30.8 x 10^3 rad s^{-1} and 18.2 m s^{-1}, respectively. The slower striking sister-species, *Aotearoa magna*, was three orders of magnitude slower in velocity and longer in duration. Histology revealed sarcomere length differences, with some muscles specialized to be slow and forceful, and others to be fast and non-forceful. 3D printed models reveal structural differences that explain how the chelicerae hinge open and closed. Combining all of this evidence I put forth a hypothesis for the ultra-fast trap-jaw mechanism. This research documents the morphological shifts that accompany ultra-fast movements and result in increased rotation in joints and increased muscle specialization.

Keywords: power-amplification; Latch Mediated Spring Actuation; LaMSA; micro-Computed-Tomography; histology; functional morphology; Arachnida.

INTRODUCTION

In animal movements, speed is often central to survival, for example, by allowing escape from a predator or the capture of prey. However, due to the intrinsic properties of muscles and the trade-off between velocity and force, muscle power is limited (Hill, 1938; Huxley, 1957). Small organisms are additionally limited due to the small size of their limbs, but have evolved ways to overcome these constraints through the use of springs, levers and latches (Gronenberg, 1996). Similar to operating a bow and arrow, biological systems have evolved where a motor, typically a muscle, slowly loads energy into an elastic structure that then is released near-instantaneously, amplifying power to produce ultra-fast movements. Arthropods in particular are notable for producing some of the fastest known animal movements and accelerations, including the mandible strikes of trap-jaw ants (Gronenberg et al., 1993; Larabee et al., 2018) and the Panamanian termite (Seid et al., 2008), and the appendage movements of mantis shrimp and snapping shrimp, both of which are so extreme that they produce a cavitation bubble (Patek et al., 2004; Versluis et al., 2000).

Power-amplified mechanisms have evolved numerous times across the tree of life and accordingly are diverse in morphology, yet they are united by the presence of several functional elements: an "engine" or motor (e.g., a muscle) that loads the "amplifier" (e.g., a spring), which when released near-instantaneously, moves the "tool" (e.g., an appendage) (Claverie et al., 2011; Patek et al., 2011). Study of these systems can enlighten our understanding of how evolution proceeds. Typically the muscle that acts as the engine is large, slow, and forceful, and the muscle that triggers the release of energy is small and fast, as seen in trap-jaw ants (Gronenberg, 1995). The link between form and function in these systems shows that minor morphological changes in joints can produce large functional differences (Kaji et al., 2018). Recent research has focused on the springs that convert potential energy into kinetic energy and the latches that control this energy flow, and these systems have been newly termed Latch-Mediated Spring Actuation (LaMSA) (Longo et al., 2019). Synthesizing knowledge across LaMSA systems reveals limitations on producing power due to cascading effects of the force-velocity trade-offs, predicts which systems are best driven by a muscle or by a spring, and ultimately informs how fabricated, biomimetic systems can be optimized and designed (Ilton et al., 2018).

Ultra-fast movements have been discovered and documented in the cheliceral strikes of Mecysmaucheniidae spiders (Wood et al., 2016), earning this group the common name “trap-jaw spiders.” Mecysmaucheniids do not build a web for prey capture, and instead are active hunters that live deep within leaf litter, logs, and moss on the forest floor, and very little is known about the natural history of these spiders. High-speed videography showed that four species, out of 14 examined, had ultra-fast cheliceral strikes, and there is considerable functional and morphological variation between species. All mecysmaucheniid species, regardless of strike speed, prior to a cheliceral strike, lift their chelicerae upwards, while rotating open, to achieve a wide gape with the chelicerae extended anterolaterally away from the body (Fig. 1A-B). During a strike the chelicerae close in the frontal plane, and are only later moved downward to their resting position close to their mouthparts. This is in contrast to the typical left-right lateral movements of most spiders where the chelicerae remain close to the body and mouthparts. A row of setae runs along and lies flat against the inner margin of the resting chelicerae, but projects anteriorly in the open chelicerae (arrow in Fig. 1A). During high-speed recordings, contact with these setae preceded a strike, similar to the trigger-hairs in trap-jaw ants (Gronenberg et al., 1993). Phylogenetic analysis of molecular sequence data uncovered that the four species with ultra-fast strikes do not form a monophyletic group, but instead represent four independent origins (Wood et al., 2016). These four species share similar external morphologies that are not present in the slower-striking species and may be central to a LaMSA/power-amplifying mechanism: the clypeus is extended and thickened; the clypeal ligaments that attach the cheliceral bases to the anterior tip of the clypeus are also thicker.

The independent origins of the ultra-fast strikes and associated morphologies make this an excellent group for examining evolutionary diversification. However, to do so it is also necessary to describe how the ultra-fast mechanism operates, that is, identify the different components of the system: the spring, the latch, and the different muscles that load the spring and unfasten the latch. This task is challenging for several reasons. First, it is difficult to collect a large series of specimens because these spiders are cryptic, occurring in leaf litter, moss, and logs on the forest floor in New Zealand and southern South America (WSC, 2020). These spiders are also small (body length around 2-5 mm, with the smallest species having the fastest cheliceral strikes), impeding manipulative *in vivo* experiments. Confounding this, knowledge of cheliceral

function in spiders is virtually non-existent and limited to a handful of anatomy studies that describe internal musculature (e.g., Brown, 1939; Palmgren, 1978; Palmgren, 1980; Whitehead and Rempel, 1959). While most arthropod joints are simple hinges that move in one plane and are operated by relatively few muscles, many arthropods have evolved creative joint solutions that allow for less restricted movement (Patek and Longo, 2018). This seems to be the case for cheliceral movements in mecysmaucheniids, which are more maneuverable compared to most other spiders. Compared to other spiders the cheliceral bases in mecysmaucheniids are surrounded by relatively large amounts of membranous tissue and are not close enough to other sclerites to restrict movement. Complicating this, in mecysmaucheniids and other spiders there are no less than nine different muscles that articulate the basal section of the chelicerae (Wood and Parkinson, 2019).

One objective of this study is to overcome these challenges and develop a hypothesis of how the ultra-fast trap-jaw mechanism functions in mecysmaucheniid spiders. In doing so I first test whether morphology predicts strike performance. In mecysmaucheniid spiders, *Zearchaea* has the fastest known cheliceral strike (Wood et al., 2016), although this study only reported average speeds due to the upper-limit of the high-speed camera's frame rate. *Aotearoa* is the closest relative to *Zearchaea* (i.e., sister-group) (Wood et al., 2018; Wood et al., 2016), and morphology suggests it has slower, non-power-amplified strikes. I gather data on functional performance using high-speed videography for these two different trap-jaw lineages known from only New Zealand. Next, I ask whether difference in functional performance correspond with differences in the internal morphology of the muscles. Synchrotron-based micro-Computed-Tomography (μCT) scanning allows for the visualization of tiny internal structures and was recently done across Palpimanoidea, including for both *Aotearoa* and *Zearchaea*, with the goal of homologizing cheliceral musculature (Wood and Parkinson, 2019). The 3D surfaces from these μCT scans are used to compare muscle and sclerite morphologies in *Aotearoa* and *Zearchaea*. I also measure sarcomere lengths in the different cheliceral muscles of the two sister lineages from histological sections. In arthropods, examining the sarcomere lengths of different muscle fibers can determine performance: muscles with long sarcomere lengths produce slow, forceful movements, while muscles with short sarcomere lengths are fast, but with low force (Blanco and Patek, 2014, and references therein). To examine muscle line of action I build two simple models of cheliceral function using 3D-printed surfaces and elastics and strings to

represent muscles and ligaments. Finally, combining all of these results, I propose and discuss a hypothesis for the trap-jaw mechanism in mecysmaucheniid spiders.

MATERIALS AND METHODS

Study System

All experiments were performed on specimens of *Aotearoa magna* and *Zearchaea* sp., both endemic to New Zealand and sister-taxa with strong branch support based on molecular sequence data (Wood et al., 2018; Wood et al., 2016). *Aotearoa* is monotypic and *Zearchaea* consists of two described species (WSC, 2020), but based on the unfinished work of R. Forster†, there are likely around 15 species. *Aotearoa magna* body length is around 3-4 mm (Forster, 1949) and *Zearchaea* is around 2 mm or less (Forster, 1955; Wilton, 1946; R. Forster, unpublished data). *Zearchaea* are cryptic and rare to collect, making it difficult to obtain a large series of adult specimens from one species for all experiments. Because of this, *Zearchaea* specimens used in this study are likely from several different species. However, *Zearchaea* species share similar carapace/chelicerae morphology and likely are functionally similar in their predatory strikes. Spiders were collected by sifting moss and leaf litter (see Supplementary Information for collection locality). Specimens were maintained in 1 cm diameter glass vials with damp cotton in the bottom and with dry cotton plugging the opening. Vials were kept in a refrigerator with a glass door (for natural daylight cycles) and maintained at cool temperatures (around 9° C).

High-Speed Video and Analysis

Wood et al (2016) recorded *Zearchaea* at 40,000 frames s^{-1}, and did not include *Aotearoa* in the study. In Wood et al *Zearchaea* cheliceral strikes were averaged across the entire strike (i.e., speeds and durations were calculated from two positions, open and closed) because at 40K frames s^{-1} there was not enough data to calculate instantaneous velocity throughout the strike. For the current study, using a Photron FastCam Mini AX200 and a Sigma 105 mm lens, cheliceral strikes were recorded at 1K frames s^{-1} for *Aotearoa magna* and at 80K–100K frames s^{-1} for *Zearchaea* sp. These frame rates were sufficient for tracking cheliceral movement across the entire cheliceral strike. During recording, the specimen was contained in a glass tube while an eyelash, affixed to an insect mounting pin, was used to stimulate the specimen in order to

elicit a cheliceral strike. To minimize injury specimens were not affixed to a mount and were free to wander, and so most recordings are slightly off center from the dorsal view, causing one chelicera to be foreshortened (Fig. 1A-B), and the kinematic differences observed between the left and right chelicera (Fig. 1C-D) are likely due to camera angle. *Aotearoa* specimens lunged their bodies forward while striking. The 'Template Matching and Slice Alignment' plugin (available at: https://sites.google.com/site/qingzongtseng/template-matching-ij-plugin) was used in the image analysis software Fiji (Schindelin et al., 2012) to remove *Aotearoa* translational movements so that only rotational movements of the chelicera remained. Cheliceral strikes were digitized by tracking the x-y coordinates of the distal anterior edge of each chelicera using the 'point tool' in Fiji. Using R software (R Core Team, 2016), following the R-script from Larabee et al. (2018), and using the 'Pspline' package, cumulative cheliceral displacement was fit with a quantic spline and angular velocity and acceleration were calculated as the first and second derivative of the fitted displacement curve. Linear velocity was also calculated from the arc length traveled by the distal point on the chelicera and linear acceleration was calculated as linear velocity/time.

Treating each chelicera as a thin rod of uniform density that rotates around a fixed point, for each chelicera the following calculations were made. The moment of inertia, I, was calculated as:

$$I = \frac{1}{3}ML^2$$

where M and L are the chelicera mass and length, respectively. The kinetic energy of the chelicera, E, was calculated from:

$$E = \frac{1}{2}I\omega^2$$

The power of the strike, P, is calculated as:

$$P = \frac{E_{max}}{t_{E,max}}$$

where E_{max} is the maximum energy of the chelicera, and $t_{E,max}$ is the time when E is at the maximum. The power output, O, of the cheliceral strike is:

$$O = \frac{P}{m}$$

where *m* is the adductor muscle mass. Time values were based on the frame rate used for the high-speed video recordings. Cheliceral length was measured using a M205C Leica microscope. The chelicera mass and adductor muscle mass were approximated based on data from Wood et al. (2016) which reported measurements of cheliceral length, cheliceral mass, and cheliceral muscle mass, for 14 different mecysmaucheniid species. Using these data, a regression line was fit using the linear model command ('lm') in R for the natural logs of: cheliceral mass versus cheliceral length (sample size = 43 specimens, statistically significant at p-value < 0.001, Fig. S1); cheliceral total muscle mass versus cheliceral length (sample size = 14 specimens, statistically significant at p-value < 0.001, Fig. S2). Then, for *Aotearoa* and *Zearchaea* specimens, cheliceral mass and cheliceral total muscle mass was interpolated based on cheliceral length. Cheliceral adductor mass was approximated to be 75% of total cheliceral muscle mass, an estimation based on muscle volumes from the *Zearchaea* µCT scan, but an overestimation for *Aotearoa*, and so a more conservative approach.

Histology

Spider chelicerae are composed of two different sections, a basal section (the paturon) that articulates with the carapace, and a distal section composed of a fang that opens and closes against the paturon. This study focuses only on the basal joint that moves the paturon, as it is the primary joint for producing trap-jaw movements. To measure sarcomere lengths for each cheliceral muscle the cephalothorax of one *Aotearoa magna* specimen and one *Zearchaea* sp. specimen was sectioned, stained, and mounted to slides by Laudier Histology (New York, NY). Specimens were originally collected and preserved in 75% ethanol (see Supplementary information for collection data). In preparation for sectioning, specimens were transferred out of 75% ethanol and fixed with an alcoholic formalin and were slowly dehydrated by placement in ethanol of increasing concentration. The cephalothorax was then embedded in a hydrophobic acrylic resin. Using a heavy-duty rotary microtome, 2 µm sections were cut and placed on silane-coated slides. Tissue sections were deplasticized and stained with 0.1% toluidine blue for analysis. Slides were examined and photographed using an Olympus BX63F compound fluorescent microscope. Sarcomere length was measured taking five measurements per muscle, and reported as an average.

3D Morphological Visualization

Using µCT scans of *Aotearoa magna* and *Zearchaea* sp. from Wood & Parkinson (2019), different cheliceral/cephalothorax structures were digitally labeled ("segmented") and converted to a surface mesh with the purpose of homologizing the cheliceral muscles that operate the paturon within Palpimanoidea. In the current study, I follow the naming conventions and color-coding of Wood & Parkinson (2019) for each of the nine homologous cheliceral muscles (Table 1, Fig. 2, and see figs. 4 and 5 of Wood & Parkinson, 2019). For simplicity, whenever an individual muscle is discussed it will be followed in parentheses with the color code used in Table 1 and the figures.

Using Avizo software, to quantify morphological differences the following measurements were taken, and for paired structures, measurements were taken for both the left and right side and averaged: carapace width (measurement of size); clypeal ligament length; clypeal ligament thickness; clypeus length; ratio of clypeus thickness to carapace thickness (carapace thickness was measured on cuticle between anterior median eyes); carapace length; carapace height; chelicera width (taken from the middle of the long axis); chelicera length; width of sclerotized circle surrounding cheliceral bases (carapace foramen); height of foramen; and for each muscle, the cross-sectional-area, volume, and a measurement of the angle formed where all fibers converged at the apodeme, thus depicting the degree the fibers fanned out. All cheliceral muscles that operate the basal section of the chelicerae had a fusiform connection (i.e., had a narrow tendon) and were convergent (i.e., fan-shaped) in architecture, although some muscles were nearly parallel, and others more convergent. For all muscles the cross-sectional-area was estimated from µCT by: 1) taking an average of the number of fibers on the left muscle and the right muscle; 2) measuring the area of three different fibers on both the left and right muscle and then taking the average of the six; 3) and then multiplying the average number of fibers by the average fiber area.

µCT scans from Wood & Parkinson (2019) were taken on specimens with the chelicerae in the "resting" position, i.e. held down against the mouthparts (Fig. 3D,I). To understand the trap-jaw mechanism, knowledge of the position of the different muscles is also needed when the chelicerae are "open", i.e., immediately prior to a strike when the chelicerae have a wide gape, and when "closed", i.e., immediately after a strike when the closed chelicerae remain lifted. To examine the position of each muscle in the "open" and "closed" positions, using Avizo software,

landmarks were placed at apodeme attachment points on the cheliceral bases and on the carapace where the cheliceral muscles attached. Based on high-speed videos, cheliceral surfaces (with landmarks) were positioned relational to the carapace so that they approximated the "open" (Fig. 4C,G) and "closed" (Fig. 4D,H) positions. Using Adobe Illustrator, in the dorsal view and in the "resting", "open" and "closed" positions, lines were drawn connecting cheliceral landmarks to carapace landmarks to approximate the position of each muscle in the three different cheliceral position. Using these images, muscle lines of action (represented as arrows), pivot points, and lever arms were drawn to approximate the cheliceral movements caused by the different muscles.

3D Model

To examine the line of action of each muscle and the position of sclerotized structures, an enlarged 3D model was built for *Aotearoa magna* and *Zearchaea* sp. Using ABS plastic, surfaces of the following structures were printed on a Stratasys uPrint SE Plus 3D printer for *Zearchaea*, and for *Aotearoa*, were printed by makexyz, an online 3D printing on demand company: chelicerae, carapace and cheliceral sclerites (i.e., inter-cheliceral-sclerite and "triangular" sclerite). Holes were drilled into the chelicerae where tendons and ligaments attached and into the carapace, where ligaments attached and at the approximate center of the muscle attachment. Strings or elastic thread was used to represent muscles and ligaments.

RESULTS

Kinematics

A total of 21 high-speed videos of cheliceral strikes were made for *Aotearoa magna* and 11 for *Zearchaea* spp. (four from this study and seven from Wood et al., 2016). In all observations the specimens started with the chelicerae in a resting position (Fig. 3D,I), then, prior to a strike, the chelicerae move upward and open and remain extended anterolaterally away from the body (Fig. 4C,G). *Aotearoa* had an average gape of 93.6º ± 15.2 (sample size = 21) and *Zearchaea* had an average gape of 173.9º ± 11.4 (sample size = 11). Immediately after a strike, the chelicerae project anterior-medially away from the body (Fig. 4D,H). The chelicerae moved synchronously in the high-speed recordings. Because some videos were out of focus, or the chelicerae moved out of frame, or the camera was oriented in the wrong position, only a subset of the total high-speed videos were used for kinematic analysis (Table 2): 19 videos from two

individuals of *Aotearoa* (both males) and five videos from two individuals of *Zearchaea* (one penultimate female and one female) (see Supplementary Information for xy coordinates of videos and R-scripts). The variables listed in Table 2 were first averaged per video for the left and right chelicera, and then averaged for all videos. For *Aotearoa*, strike duration was 0.0191 ± 0.0052 s (mean ± standard deviation), but *Zearchaea* was three orders of magnitude shorter with a duration of 0.0843 ± 0.017 ms. Peak angular velocities were 64.8 ± 22 rad s^{-1} for *Aotearoa* and 25.0 ± 4.8 x 10^3 rad s^{-1} for *Zearchaea*, with peak linear accelerations on the order of 1.1 g for *Aotearoa* and 41K g for *Zearchaea*. The average mass-specific power output of the cheliceral strike was 0.27 ± 0.18 W kg^{-1} for *Aotearoa*, and 6.7 ± 3.4 x 10^5 W kg^{-1} for *Zearchaea*, which greatly exceeds the maximal power output for a muscle (Josephson, 1993). The fastest observed *Zearchaea* strike had a peak angular velocity of 30.8 x 10^3 rad s^{-1}, a peak linear velocity of 18.2 m s^{-1}, and a duration of 0.07 ms.

Measurements

Carapace width was treated as a measurement of size and used to scale other measurements by making a ratio (Table 3). When scaled by size, clypeal ligaments were about three times thicker (0.034 versus 0.011) and about 60% shorter (0.15 versus 0.25) in *Zearchaea* than *Aotearoa*. The clypeus was also longer and thicker (three times as thick as the carapace cuticle in *Zearchaea* and about 1.3 times as thick in *Aotearoa*). The chelicerae, when scaled by size, were longer and wider in *Aotearoa* than in *Zearchaea.*

Zearchaea has three fewer cheliceral muscles than *Aotearoa*: the anterior medial inner (blue in Fig. 2) and outer (light blue) muscles and the endosternite muscles (light orange) are absent. Relative to the total cheliceral muscle volume (calculated for only the muscles present in both *Aotearoa* and *Zearchaea*), the lateral anterior (yellow), anterior outer (red), posterior medial (green), and the inter-cheliceral-sclerite (aqua) muscles are a smaller percentage of total muscle volume in *Zearchaea* compared to *Aotearoa* (Table 4). On the other hand, the lateral posterior (magenta) muscles are a slightly greater percentage of total volume in *Zearchaea* (4% vs 1% in *Aotearoa*), and the anterior medial muscles (purple) are a much greater percentage (76% vs 32% in *Aotearoa*). Even though *Aotearoa* (carapace width = 1.1 mm) is about twice as large as *Zearchaea* (carapace width = 0.59 mm), the anterior medial muscles (purple) in *Zearchaea* have nearly the same cross-sectional area (0.044 versus 0.048 mm^2). In *Zearchaea*, three muscles have

a greater architecture angle (i.e., a more fanned-out shape) than *Aotearoa* (the lateral anterior muscles, yellow; the anterior outer muscles, red; and the anterior medial muscles, purple) and three muscles have a smaller angle (i.e., a more parallel shape) than *A.* (the posterior medial muscles, green; the inter-cheliceral-sclerite muscles, aqua; and only slightly in the lateral posterior muscles, magenta).

Histology

There were differences in sarcomere lengths among different muscles (Table 4; Fig. S3). Within a muscle, in *Zearchaea* different fibers had similar sarcomere lengths, however, in *Aotearoa*, two muscles (the lateral posterior, magenta, and the inter-cheliceral-sclerite, aqua) had two different fiber types, one with shorter sarcomeres and one with longer. The inter-cheliceral-sclerite muscles (aqua) in *Zearchaea* had the shortest sarcomeres (2.49 ± 0.42 µm, mean ± standard deviation; Fig. S3D) and this muscle was also relatively smaller (1.5% total muscle volume versus 8.5% in *Aotearoa*). In both taxa this muscle was oriented more perpendicular to the other muscles and to the plane of movement as the chelicerae went from open to closed (Fig. 4B,F). In *Aotearoa* this relatively larger muscle consists of two different fiber types: fibers with the longest sarcomeres and fibers with the shortest sarcomeres (6.11 ± 0.57 µm and 2.79 ± 0.20 µm, respectively; Fig. S3B). In both taxa, the anterior medial muscles (purple) consist of only one fiber type and have long sarcomeres compared to the other muscles (4.80 ± 0.65 µm in *Aotearoa* and 5.23 ± 0.38 µm in *Zearchaea*; Fig. S3A,C-D). The remaining muscles in both taxa have sarcomere lengths that are mostly around 3-4 µm (Fig. S3C), although with some exceptions (e.g., the short sarcomeres in the posterior medial muscles, green, in *Zearchaea*).

Lever Arms and Torque

Examination of the high-speed videos suggests that the chelicerae are anchored at and pivot around the anterior, lateral, basal corner (i.e., the fulcrum position), which coincides with where the clypeal ligaments attach (Fig. 3B-C,G-H). Using 2D images of the chelicerae in the "resting", "open", and "closed" position (Fig. S4), muscle forces (represented as arrows), fulcrums (at the juncture between the cheliceral base and the clypeal ligament), and lever arms were placed to approximate the cheliceral movements that would be caused by contraction of different muscles. Out of all nine muscles (Table 1, Fig. 2), only the anterior outer muscles (red)

were positioned to produce cheliceral abduction (Fig. 3). These muscles attach to the anterior lateral corners of the cheliceral bases (close to the fulcrum) and run diagonally back to attach to the carapace (Fig. 3C-E,H-J). In the anterior view (Fig. 3C,H) contraction of these muscles likely increases the cheliceral gape. In the dorsal view, contraction causes the chelicerae to rotate outwards so that the posterior edge of the chelicerae moves forward (Figs. 3E,J) and lifts up. In *Zearchaea* relative to *Aotearoa*, the anterior outer muscles (red) attach further from the fulcrum, so that the lever arm is relatively longer (compare Figs. 2A and 3C-E with 2B and 3H-J), thereby increasing the torque. All remaining eight muscles, based on their position, likely would adduct or depress the chelicerae in both taxa.

Hand-Held Model

The 3D printed model provided additional information about cheliceral function (see Supplementary Videos). First, the clypeal ligaments are necessary to anchor the chelicerae: without a tight anchor, when the different muscles (represented as strings) were pulled, the cheliceral bases would move backwards into the carapace. With the clypeal ligaments in place (i.e., tight strings or tight elastic), pulling on the strings that represent the anterior outer muscles (red) caused the chelicerae to elevate, open, and rotate outwards (i.e., pitch backwards) in both *Aotearoa* and *Zearchaea*. Although this movement often required a slight initial push from behind the cheliceral bases to initiate movement, and also a final push in *Zearchaea* to achieve the wide-gape.

Second, in both *Aotearoa* and *Zearchaea*, the cheliceral bases have a constriction that interacts with the carapace foramen (i.e., the hole that completely surrounds the cheliceral bases; see Fig. 3). The lateral edges of the foramen in the 3D model fits into a groove on the cheliceral bases and likely guides abduction (Fig. 5B).

Third, in *Aotearoa*, the shape of the inter-cheliceral-sclerite (orange in Figs. 2A and 3E) had a tight fit with the cheliceral bases and created a hinge that stabilized the cheliceral bases as they hinged open around the posterior projections (Fig. 5A). In *Zearchaea*, the inter-cheliceral-sclerite also formed a hinge for the cheliceral bases, but this hinge had greater flexibility, allowing the chelicerae to open nearly 180° (Fig. 5B). Because of the elongated clypeus in *Zearchaea*, the clypeal ligaments have a different angle of attachment to the cheliceral bases in each taxon (Figs. 2, 3E,J). In *Zearchaea*, the hinge formed by the inter-cheliceral-sclerite was bi-

stable (similar to a “snap clip” used to secure hair), so that it wants to be either open or closed and is unstable in-between. This is due to the tight anchoring of the clypeal ligaments, so that as the chelicerae pass through intermediate positions, there is either compression of the cheliceral-bases/inter-cheliceral-sclerite hinge, or stretching of the clypeal ligaments, or a combination of both. In *Aotearoa* the average gape (93.6º, compared to 173.9º in *Zearchaea*) is not wide enough that the chelicerae open in the same way.

Fourth, with the chelicerae in the open position, pulling on the strings that represent all remaining muscles (other than the anterior outer muscles, red) caused the chelicerae to adduct and/or depress. The anterior medial strings (purple) also caused the open chelicerae to pitch backwards. With the exception of the inter-cheliceral-sclerite muscle (aqua), all cheliceral muscles attach to the cheliceral bases and pulling on either the left or right side resulted in uneven cheliceral movement. On the other hand, the inter-cheliceral-sclerite muscle (aqua) connects to the inter-cheliceral-sclerite that sits between and creates a hinge with the cheliceral bases (Figs. 2, 4B,F). When the strings that represented this muscle were pulled, the chelicerae closed in unison.

Lastly, in *Zearchaea*, there is an additional sclerite that is not present in *Aotearoa* (the “triangular sclerite”, Fig. 5B and see fig. 5c,l,o in Wood & Parkinson, 2019) that sits ventral to the inter-cheliceral-sclerite. The uppermost tip of the triangular sclerite comes into contact with a groove on the lower edge of the inter-cheliceral-sclerite in the 3D model when the chelicerae are open (Fig. 5B). In *Zearchaea*, after opening the chelicerae with the anterior outer strings (red), the anterior medial strings (purple) could be pulled followed by pulling the inter-cheliceral-sclerite strings (aqua), which caused the chelicerae to snap closed. If the anterior outer strings (red) were not released when the chelicerae closed, the chelicerae remained lifted up in the closed position.

DISCUSSION

Kinematics

Cheliceral strikes in *Zearchaea* are the fastest known arachnid movement to date, with the greatest accelerations in the shortest durations. Because *Zearchaea* are difficult to collect, especially alive, high-speed videography was performed using only one penultimate (one molt away from adult) specimen (recorded at 80K and 100K frames s^{-1}) and one adult specimen (from

a previous study, recorded at 40K frames s^{-1}). Both specimens, based on their locality (R. Forster†, *unpublished data*) are likely different species. However, all *Zearchaea* morphospecies share similar carapace/chelicerae morphology, and most likely achieve similar speeds in their predatory strikes. Based on external morphology (reduced clypeus and clypeal ligaments), *Aotearoa* was hypothesized to be slow-striking and was shown in this study to be three orders of magnitude slower in velocity and longer in duration. This suggests that for mecysmaucheniid spiders external morphology can be used to predict cheliceral velocity.

Muscle Morphology

One objective of this study was to test whether difference in functional performance also correspond with differences in muscle morphology. Results suggest evidence of specialization in muscles in the two sister-lineages. Documented in Wood & Parkinson (2019), *Aotearoa* has a complete set of cheliceral muscles (nine total) similar to its close relatives (Palpimanoidea), while in *Zearchaea*, three muscles (anterior medial inner, blue; anterior medial outer, light blue; endosternite muscle, light orange) are absent. Ultra-fast cheliceral strikes are hypothesized in *Zearchaea* to operate via LaMSA: while muscles put energy into the elastic system and cause the release of the latching mechanism, closure is not directly driven by muscles. In *Zearchaea* some of the closure muscles may have become unnecessary and were lost. A species with a complete set of muscle, over geological timescales may have more evolutionary flexibility, whereas a species with fewer muscles may have less potential to diversify.

By examining the physical properties of a muscle we can observe shifts in muscle specialization. In mecysmaucheniids, the different cheliceral muscles are all fan-shaped, that is, have a narrow tendon that attaches to the cheliceral bases and with the fibers then spreading out in their attachment to the carapace, although there is variation in the degree the fibers fan out, with some muscles being nearly parallel. Fan-shaped muscles produce greater forces and are more versatile as the contraction of different fibers can change the direction the muscle pulls; in contrast, muscles with more parallel fibers (e.g., strap shaped) have faster contractions and can cause a greater degree of movement (Walker and Liem, 1994). In *Aotearoa*, contraction of the inter-cheliceral-sclerite muscles (aqua) likely pulls the chelicerae closed via the inter-cheliceral-sclerite, whereas in the ultra-fast *Zearchaea*, contraction of this muscle pulls the ICS backwards, destabilizing the cocked system by releasing the latch and triggering the release of the chelicerae.

In this LaMSA mediated system the inter-cheliceral-sclerite muscle (aqua) is narrower so that the fibers run more parallel (*Zearchaea* muscle shape angle is 69°, and *Aotearoa* is 108°). This architecture implies that this muscle is more specialized for speed in the ultra-fast *Zearchaea* and slower, yet more versatile in slower-striking *Aotearoa*. Furthermore, the inter-cheliceral-sclerite muscle (aqua) is composed of two fiber types in *Aotearoa* (fibers with short sarcomeres and fibers with long sarcomeres; Fig. S3B), but in *Zearchaea* this muscle appears to only have fibers with short sarcomeres (Table 4). This is similar to what has been observed in ants, where it is the relative proportion of fast fibers (short sarcomeres) to slow fibers (long sarcomeres) that determines mandible velocity (Gronenberg et al., 1997). It is the opposite scenario for the anterior medial muscles (purple), which are hypothesized to slowly and forcefully put energy into the high-speed LaMSA system. In the ultra-fast system the anterior medial muscles (purple) have a wider degree of fanning out (*Zearchaea* muscle shape angle is 64°, and *Aotearoa* is 39°), which implies that relatively, this muscle shape is more specialized for producing larger forces. The longer sarcomeres in this muscle also suggests that in the LaMSA system this muscle is comparatively more specialized for slow, forceful movements.

Hypothesis for Trap-Jaw Mechanism

Combining all of the results from this study, I propose a hypothesis for the trap-jaw mechanism in mecysmaucheniid spiders. Cheliceral strike movements appear to be produced primarily by three muscles:

(1) Contraction of the anterior outer muscles (red) causes the chelicerae to lift up, open, and pitch backwards. In *Zearchaea*, there is greater torque for opening the relatively smaller chelicerae because of the longer lever arm. In *Aotearoa*, while the anterior outer muscles (red) are positioned to produce cheliceral opening, it is hard to believe that these muscles alone, with their short lever arms (Figs. 2A and 3C-E), can generate the torque necessary to lift the larger, more robust chelicerae, implicating hydraulic pressure (see discussion below).

(2) Contrary to the asynchronous, ultra-fast mandible movements observed in *Odontomachus* trap-jaw ants (Patek et al., 2006), in mecysmaucheniids, the chelicerae have always been observed to close in unison (Wood et al., 2016, and current study). For muscles that attach to the cheliceral bases, synchronous movement would require coordinated contraction of the left and right side within milliseconds. Alternatively, the inter-cheliceral-sclerite muscles

(aqua) connect to a sclerite that sits between and forms a hinge with the cheliceral bases (Figs. 2, 4B,F). Contraction of this muscle in the 3D model pulls the inter-cheliceral-sclerite into the cephalothorax, pulling each chelicera along with it in unison. In both taxa this muscle is oriented more vertically compared to the other cheliceral muscles (Fig. 4B,F) and is perpendicular to the plane of movement as the chelicerae close (in Fig. 4C,D,G,H). In *Zearchaea*, this muscle has the shortest sarcomere lengths (average 2.49 µm) and it is relatively smaller in volume. All of this evidence suggests that in *Zearchaea* this is a fast, low-force muscle, whose contraction moves the inter-cheliceral-sclerite, triggering the rapid destabilization of the system and nearly-instantaneously releasing stored energy. In contrast, in *Aotearoa*, this muscle has a mix of fibers with shorter sarcomeres (2.79 ± 0.20 µm, mean ± standard deviation) and with the longest sarcomeres (6.11 ± 0.57 µm), so that this muscle is more versatile, but still, due to its position, is likely the muscle primarily responsible for initiating synchronous chelicera closure.

(3) Contraction of the anterior medial muscles (purple) pulls the inner cheliceral margins backwards, and would cause the open chelicerae to close. This muscles is slow and forceful, having some of the longest sarcomere lengths in both taxa compared to other muscles. This muscle is also markedly larger in *Zearchaea* compared to *Aotearoa.* In *Zearchaea*, this large closure muscle is likely the "engine" that provides energy into the latch/spring (LaMSA) trap-jaw mechanism. Contraction of this muscle in the latched-open chelicerae of *Zearchaea*, pitches the chelicerae back, thereby stretching the clypeal ligaments and storing energy into the "spring" for the ultra-fast strike (Fig. 4G). I hypothesize that the clypeal ligaments act as the amplifier because they are so thick in *Zearchaea* and because they attach to the clypeus, which is also thick and darkly sclerotized. In high-speed videos there is not obvious compression of the clypeus or the carapace, but the low resolution of the videos makes this difficult to determine. In *Aotearoa*, the slow, forceful anterior medial muscles (purple) may work together with other closure muscles: the anterior medial inner and outer muscles (blue and light blue, Fig. 4A,C), both of which are absent in *Zearchaea*, and the inter-cheliceral-sclerite muscle (aqua). Coordination and contraction of all of these muscles in *Aotearoa* may allow the chelicerae to squeeze together with great strength for holding captured prey.

The three muscles detailed above seem to be central to the trap-jaw cheliceral strike. However, these muscles are only a subset of the nine total cheliceral muscles, which leads to the question of the purpose of the remaining cheliceral muscles. The chelicerae are vitally important

to spider biology, and other than prey capture and immobilization via venom injection, spiders use their chelicerae for many other tasks involving grasping and manipulating objects. Examples of such tasks include prey manipulation, grooming, cutting silk threads, mating rituals where different appendages are clasped, burrowing, and carrying egg cases. The trap-jaw strike has a stereotyped fixed pattern of movement, and it could be that these other muscles are used for other, more general movements crucial for spider survival. Additionally, these other muscles might produce nuanced movements in the trap-jaw strike that complement the function of the three muscles discussed above.

The slower strike of *Aotearoa*: The predatory strike does not appear to involve a latch/spring mechanism for storing energy. Contraction of the anterior outer muscles (red) causes the chelicerae to rotate outwards and lift up. The fixed pattern of cheliceral movements in both *Aotearoa* and *Zearchaea* appears to be anchored and stabilized by the clypeal ligaments, and, during opening, appears to be guided by the lateral edge of the carapace foramen that interacts with the groove on the cheliceral bases. In *Aotearoa* the inter-cheliceral-sclerite (ICS) forms a hinge with the cheliceral bases and guides the movement. The ICS muscles (aqua) initiates synchronous cheliceral closure, and may work in combination with other muscles (the anterior medial muscles, purple, and the anterior medial inner and outer muscles, blue and light blue) to squeeze the chelicerae closed with a strong grip. There does not seem to be a latch that holds the chelicerae open, although hydraulic pressure (see below) may be involved in lifting the chelicerae and maintaining them open.

The ultra-fast strike of *Zearchaea:* Contraction of the anterior outer muscles (red) abducts the chelicerae to their open position. The ICS sits between the cheliceral bases and forms a hinge that seems to be stable when the chelicerae are in both the “resting” and “open” position due to the tight clypeal ligaments. This bi-stability may help latch the chelicerae open. A triangular sclerite (absent in *Aotearoa*) may also help in latching the chelicerae open, although this sclerite has no associated muscles. The triangular sclerite sits beneath the ICS and appears to fit into a groove on the ICS. With the chelicerae in the open position, the anterior medial muscles (purple) slowly and forcefully begin to contract, causing the open chelicerae to pitch backwards, thereby stretching of the clypeal ligaments, the “spring” that stores elastic potential energy. This

backward pitch of the chelicerae may further enable latching/locking of the open chelicerae by moving the ICS more forward. To strike, the fast ICS muscles (aqua) contract and pull the ICS backwards, destabilizing the system and causing rapid release of stored energy as the chelicerae are flung forward.

Evidence for Hydraulic Pressure in Cheliceral Movements

Hydraulic pressure plays a significant role in spider biology as it is necessary for tasks crucial to spider survival and reproduction. In spider locomotion, extensor muscles are missing in several leg joints and leg extension is instead caused by increasing the hemolymph pressure in the legs via contraction of prosomal muscles (Shultz, 1991). During copulation, hydraulic pressure is used to inflate the sclerites in the male secondary genitalia so that they can couple with the female genitalia (Eberhard and Huber, 2010). It is currently unknown whether hydraulic pressure also plays a role in cheliceral movements, but it is documented that spiders maintain their bodies at high pressures (Kropf, 2013), and hydraulic pressure has been implicated in the oscillating cheliceral movements of spitting spiders, Scytodidae (Suter and Stratton, 2013). The significance of hydraulic pressure to spider biology raises the possibility that hydraulic pressure may also be utilized for operating the trap-jaw movements in mecysmaucheniids.

Mecysmaucheniids have highly maneuverable chelicerae, including the ability to lift their long chelicerae up and hold them extended, away from their mouthparts, compared to the typical left-right lateral movements of other spiders. In most spiders the chelicerae are wedged between the carapace and the mouthparts (endites, labrum), but in mecysmaucheniids, the modified carapace completely encircles the cheliceral bases. There is a large space of soft, membranous cuticle between the carapace foramen and the cheliceral bases, likely contributing to the increased maneuverability. In spite of their maneuverable nature, during a predatory strike the chelicerae still follow a set line of movement, likely due to the clypeal ligaments. Were it not for the clypeal ligaments, which anchor the anterior lateral corner of the cheliceral bases, contraction of any cheliceral muscles would pull the chelicerae back into the cephalothorax because of the soft membrane surrounding the cheliceral bases. This fulcrum allows the cheliceral bases to hinge open and rotate outward prior to a strike. Yet, immediately after closure (i.e., the “closed” position of Fig. 4D,H) the chelicerae still remain lifted up. There do not appear to be muscles present in the right orientation that could elevate the closed chelicerae. Although, it may be the

anterior outer muscles (red) remain contracted during closure, which could contribute to elevation.

An alternative hypothesis of the trap-jaw cheliceral strike may involve hydraulic pressure, which may work in combination with the anterior outer muscles (red) to push the cheliceral bases outward during opening, in maintaining the open position prior to a strike, and also in keeping the closed chelicerae lifted immediately after a strike. The chelicerae of *Aotearoa* are relatively more robust, being both longer and wider when scaled by size (Table 3), and the effort arm for the anterior outer muscles (red) is shorter. For *Aotearoa*, the shorter effort arm, and the larger load, would require greater muscle force to lift the chelicerae (mechanical advantage: *Aotearoa* = 0.012, *Zearchaea* = 0.047). For both taxa, this lever is mechanically disadvantaged and hydraulic pressure on the cheliceral bases would help with lifting the chelicerae. In the 3D hand-held models of both taxa, but particularly *Aotearoa*, pulling on the strings that represent the anterior outer muscles (red) only causes opening if the chelicerae are already slightly open. Hydraulic pressure would help open the chelicerae by pushing the posterior portion of the cheliceral bases forward (grey arrow in Fig. 3E,J), and would keep them forward and lifted during and after closure. This line of reasoning is not direct evidence, but is suggestive that another force besides that from the anterior outer muscles (red) may be needed for lifting and opening the chelicerae.

Conclusions

The ultra-fast trap-jaw mechanism in mecysmaucheniids is very different in morphology compared to other known systems that rely on latches and springs to rapidly release stored energy (e.g., LaMSA or power-amplification). In mecysmaucheniid spiders there are nine different sets of cheliceral muscles that produce intricate movements in multiple degrees of freedom, and this is confounded by the current lack of knowledge regarding cheliceral function in spiders. Yet, with the new findings presented in this study, it is apparent that in other ways mecysmaucheniid spiders are similar to other LaMSA systems, confirming fundamental patterns of evolution. Like other latch/spring systems, the mecysmaucheniid trap-jaw mechanism is composed of three main elements: the “engine”, the “amplifier” and the “tool” (Claverie et al., 2011; Patek et al., 2011). Similar to the closure muscle in other latch/spring systems, the “engine” is a large, slow, forceful muscle, and the trigger is a smaller, faster, and lower-force

muscle (Gronenberg, 1995; Ritzmann, 1974). Similar to the snapping-shrimp, this study offers another example of how morphological shifts have resulted in the increased rotation in joints that accompanies evolution of ultra-fast movements (Kaji et al., 2018). Findings regarding relative sarcomere lengths, muscle architecture, loss of and specialization in muscles, all make sense given our understanding of other LaMSA systems. The next step in this research is to take what was learned here and begin to examine form and function across additional mecysmaucheniid lineages.

ACKNOWLEDGEMENTS

Thanks to Jeffrey Shultz, Sheila Patek and her lab, Fred Larabee, Luke Macaulay, Robert Kallal, and Gustavo de Miranda for discussion, Tom Nguyen for assisting with high speed videos, and two anonymous reviewers for their comments.

COMPETING INTERESTS

No competing interests declared.

FUNDING

Fieldwork to collect specimens in New Zealand was funded by a Global Genome Initiative grant (GGI-Peer-2018-181) and a Small Grant award (year 2016) from the National Museum of Natural History. Histology and 3D printing were funded by a Core Research Grant (year 2019) from the Associate Director for Science, NMNH.

DATA AVAILABILITY

XY coordinate data for performing kinematic analysis of high-speed videos and associated R scripts will be made publicly available after acceptance.

REFERENCES

Blanco, M. M. and Patek, S. (2014) Muscle trade-offs in a power-amplified prey capture system. Evolution 68, 1399-1414.

Brown, R. B. (1939) The musculature of *Agelena naevia*: Journal of Morphology 64, 115-166.

Claverie, T., Chan, E. and Patek, S. N. (2011) Modularity and scaling in fast movements: power amplification in mantis shrimp. Evolution 65, 443-461.

Eberhard, W. G. and Huber, B. A. (2010) Spider genitalia. In *The evolution of primary sexual characters in animals* (eds. J. Leonard and A. Cordoba-Aguilar), pp. 249-284. Oxford, Oxford University Press.

Forster, R. R. (1949) New Zealand spiders of the family Archaeidae. Records of the Canterbury Museum 5, 193-203.

Forster, R. R. (1955) Spiders of the Family Archaeidae from Australia and New Zealand. Transactions of the Royal Society of New Zealand 83, 391-403.

Gronenberg, W. (1995) The fast mandible strike in the trap-jaw ant *Odontomachus.* I. Temporal properties and morphological characteristics. Journal of Comparative Physiology A 176, 391-398.

Gronenberg, W. (1996) Fast actions in small animals: springs and click mechanisms. Journal of Comparative Physiology A 178, 727-734.

Gronenberg, W., Paul, J., Just, S. and Hölldobler, B. (1997) Mandible muscle fibers in ants: fast or powerful? Cell and tissue research 289, 347-361.

Gronenberg, W., Tautz, J. and Hölldobler, B. (1993) Fast trap jaws and giant neurons in the ant *Odontomachus*. Science 262, 561-563.

Hill, A. V. (1938) The heat of shortening and the dynamic constants of muscle. Proceedings of the Royal Society of London, Series B-Biological Sciences 126, 136-195.

Huxley, A. F. (1957) Muscle structure and theories of contraction. Prog. Biophys. Biophys. Chem. 7, 255-318.

Ilton, M., Bhamla, M. S., Ma, X., Cox, S. M., Fitchett, L. L., Kim, Y., Koh, J.-s., Krishnamurthy, D., Kuo, C.-Y., Temel, F. Z., Crosby, M. P., Sutton, G. P., Wood, R. J., Azizi, E., Bergbreiter, S. and Patek, S. N. (2018) The principles of cascading power limits in small, fast biological and engineered systems. Science 360, p. eaao1082.

Josephson, R. (1993) Contraction dynamics and power output of skeletal muscle. Annual review of physiology 55, 527-546.

Kaji, T., Anker, A., Wirkner, C. S. and Palmer, A. R. (2018) Parallel saltational evolution of ultrafast movements in snapping shrimp claws. Current Biology 28, 106-113. e104.

Kropf, C. (2013) Hydraulic system of locomotion. In *Spider Ecophysiology* (ed. W. Nentwig), pp. 43-56. Springer.

Larabee, F. J., Smith, A. A. and Suarez, A. V. (2018) Snap-jaw morphology is specialized for high-speed power amplification in the Dracula ant, *Mystrium camillae*. Royal Society open science 5, 181447.
Longo, S., Cox, S., Azizi, E., Ilton, M., Olberding, J., St Pierre, R. and Patek, S. (2019) Beyond power amplification: latch-mediated spring actuation is an emerging framework for the study of diverse elastic systems. Journal of Experimental Biology 222, jeb197889.
Palmgren, P. (1978) On the muscular anatomy of spiders. Acta Zoologica Fennica 155, 1-41.
Palmgren, P. (1980) Some comments on the anatomy of spiders. Annales Zoologici Fennic 17, 161-173.
Patek, S., Dudek, D. and Rosario, M. (2011) From bouncy legs to poisoned arrows: elastic movements in invertebrates. The Journal of Experimental Biology 214, 1973-1980.
Patek, S., Korff, W. and Caldwell, R. (2004) Biomechanics: Deadly strike mechanism of a mantis shrimp. Nature 428, 819-820.
Patek, S. and Longo, S. J. (2018) Evolutionary Biomechanics: The Pathway to Power in Snapping Shrimp. Current Biology 28, R115-R117.
Patek, S. N., Baio, J. E., Fisher, B. L. and Suarez, A. V. (2006) Multifunctionality and mechanical origins: ballistic jaw propulsion in trap-jaw ants. Proceedings of the National Academy of Sciences 103, 12787-12792.
R Core Team (2016) R: A language and environment for statistical computing. R Foundation for Statistical Computing, Vienna, Austria.
Ritzmann, R. E. (1974) Mechanisms for the snapping behavior of two alpheid shrimp, *Alpheus californiensis* and *Alpheus heterochelis*. Journal of Comparative Physiology A: Neuroethology, Sensory, Neural, and Behavioral Physiology 95, 217-236.
Schindelin, J., Arganda-Carreras, I., Frise, E., Kaynig, V., Longair, M., Pietzsch, T., Preibisch, S., Rueden, C., Saalfeld, S. and Schmid, B. (2012) Fiji: an open-source platform for biological-image analysis. Nature methods 9, 676-682.
Seid, M. A., Scheffrahn, R. H. and Niven, J. E. (2008) The rapid mandible strike of a termite soldier. Current Biology 18, R1049-R1050.
Shultz, J. W. (1991) Evolution of locomotion in Arachnida: the hydraulic pressure pump of the giant whipscorpion, *Mastigoproctus giganteus* (Uropygi). Journal of Morphology 210, 13-31.
Suter, R. B. and Stratton, G. E. (2013) Predation by spitting spiders: elaborate venom gland, intricate delivery system, In *Spider Ecophysiology* (ed. W. Nentwig), pp. 241-251. Springer.
Versluis, M., Schmitz, B., von der Heydt, A. and Lohse, D. (2000) How snapping shrimp snap: through cavitating bubbles. Science 289, 2114-2117.
Walker, W. F. and Liem, K. F. (1994) *Functional Anatomy of the Vertebrates, an evolutionary perspective*. Fort Worth, Saunders College Publishing.
Whitehead, W. and Rempel, J. (1959) A study of the musculature of the black widow spider, *Latrodectus mactans* (Fabr.). Canadian Journal of Zoology 37, 831-870.

Wilton, C. (1946) A new spider of the family Archaeidae from New Zealand. Dominion Museum Records in Entomology 1, 19-26.
Wood, H. and Parkinson, D. Y. (2019) Comparative morphology of cheliceral muscles using high-resolution x-ray Computed Tomography in palpimanoid spiders (Araneae, Palpimanoidea). Journal of Morphology 280, 232-243.
Wood, H. M., González, V. L., Lloyd, M., Coddington, J. and Scharff, N. (2018) Next-Generation museum genomics: phylogenetic relationships among palpimanoid spiders using sequence capture techniques (Araneae: Palpimanoidea). Molecular Phylogenetics and Evolution 127, 907-918.
Wood, H. M., Parkinson, D. Y., Griswold, C. E., Gillespie, R. G. and Elias, D. O. (2016) Extremely rapid predatory strikes evolved repeatedly in trap-jaw spiders. Current Biology 26, 1-5.
WSC (2020) World Spider Catalog. Natural History Museum Bern, online at http://wsc.nmbe.ch, version 21.0, accessed on March 11, 2020.

TABLES

Table 1. Muscle names, colors, and numbering used throughout manuscript, based on Wood & Parkinson (2019).

Number	Color in figures	Name in present paper
i	yellow	lateral anterior
ii	magenta	lateral posterior
iii	red	anterior outer
iv	green	posterior medial
v	purple	anterior medial
vi	blue	anterior medial inner
vii	light blue	anterior medial outer
viii	aqua	inter-cheliceral-sclerite muscle
ix	light orange	endosternite muscle

Table 2. Kinematic values from high-speed video recordings. All variables are reported as mean ± standard deviation. Sample size is the total number of high-speed video available from two specimens for each lineage followed in parentheses by the number of videos per specimen.

Species	Sample size	Strike duration (ms)	Peak angular velocity (rad s^{-1})	Peak angular acceleration (rad s^{-2})	Peak linear velocity (m s^{-1})	Peak linear acceleration (m s^{-2})	Power output (watt kg^{-1})
Aotearoa magna	19 (5,14)	19.1 ± 5.2	64.8 ± 22	$7.750 \pm 3.0 \times 10^{3}$	0.0914 ± 0.031	10.9 ± 4.2	$2.70 \pm 1.8 \times 10^{-1}$
Zearchaea sp.*	5 (1,4)	0.0843 ± 0.017	$25.0 \pm 4.8 \times 10^{3}$	$6.79 \pm 2.0 \times 10^{8}$	14.9 ± 2.8	$40.1 \pm 12 \times 10^{4}$	$6.67 \pm 3.4 \times 10^{5}$

* Videos of *Zearchaea* are from two specimens that are likely different species.

Table 3. Measurements. All measurements with a (*) represent an average of the left and right side.

Species	Carapace width (mm)	Clypeal ligament length* (mm)	Clypeal ligament thickness* (mm)	Clypeus length (mm)	Clypeus thickness/ carapace thickness*	Carapace length (mm)	Chelicera length* (mm)	Chelicera width* (mm)	Carapace height (mm)	Foramen width (mm)	Foramen height (mm)
Zearchaea: actual size	0.59	0.086	0.020	0.18	3.0	0.65	0.62	0.13	0.69	0.36	0.31
Aotearoa: actual size	1.1	0.27	0.012	0.21	1.3	1.2	1.5	0.43	1.3	0.80	0.52
Zearchaea: scaled by size	1	0.15	0.034	0.31		1.1	1.0	0.23	1.2	0.61	0.53
Aotearoa: scaled by size	1	0.25	0.011	0.19		1.1	1.3	0.39	1.2	0.73	0.48

Table 4. Measurements of different cheliceral muscles in Zearchaea and Aotearoa. Averages are from two measurements taken from the left and right sides, except for average sarcomere length, which is an average of five measurements ± standard deviation. Muscle percentage volume is based only on muscles present in both taxa.

Muscle	Species	Cross-sectional area (x 10^3 mm^2)	Average volume (x 10^3 mm^3)	% of total muscle volume	Average angle (∘)	Average sarcomere length (μm)
1. lateral anterior, yellow	*Zearchaea*	5.59	1.20	0.11	51	3.48 ± 0.33
	Aotearoa	18.5	8.94	0.18	38	4.07 ± 0.44
2. lateral posterior, magenta	*Zearchaea*	1.26	0.422	0.039	27	4.08± 0.29
	Aotearoa	10.3	0.504	0.0098	34	fiber I: 2.64 ± 0.45
						fiber II: 3.87 ± 0.55
3. anterior outer, red	*Zearchaea*	0.931	0.128	0.012	21	3.58 ± 0.42
	Aotearoa	7.57	3.78	0.074	13	4.45 ± 0.39
4. posterior medial, green	*Zearchaea*	2.38	0.740	0.068	11	2.83 ± 0.069
	Aotearoa	45.3	17.0	0.33	40	3.45 ± 0.30
5. anterior medial, purple	*Zearchaea*	44.1	8.30	0.76	64	5.23 ± 0.38
	Aotearoa	48.1	16.5	0.32	39	4.80 ± 0.65
6. anterior medial inner, blue	*Zearchaea*	n/a	n/a	n/a	n/a	n/a
	Aotearoa	5.65	1.21		12	3.70 ± 0.43
7. anterior medial outer, light blue	*Zearchaea*	n/a	n/a	n/a	n/a	n/a
	Aotearoa	2.53	1.74		29	3.63 ± 0.69
8. inter-cheliceral-sclerite, aqua	*Zearchaea*	1.40	0.169	0.015	69	2.49 ± 0.42
	Aotearoa	9.74	4.39	0.086	110	fiber I: 2.79 ± 0.20
						fiber II: 6.11 ± 0.57
9. endosternite, gold	*Zearchaea*	n/a	n/a	n/a	n/a	n/a
	Aotearoa	3.19	2.07		33	3.22 ± 0.31

Figures

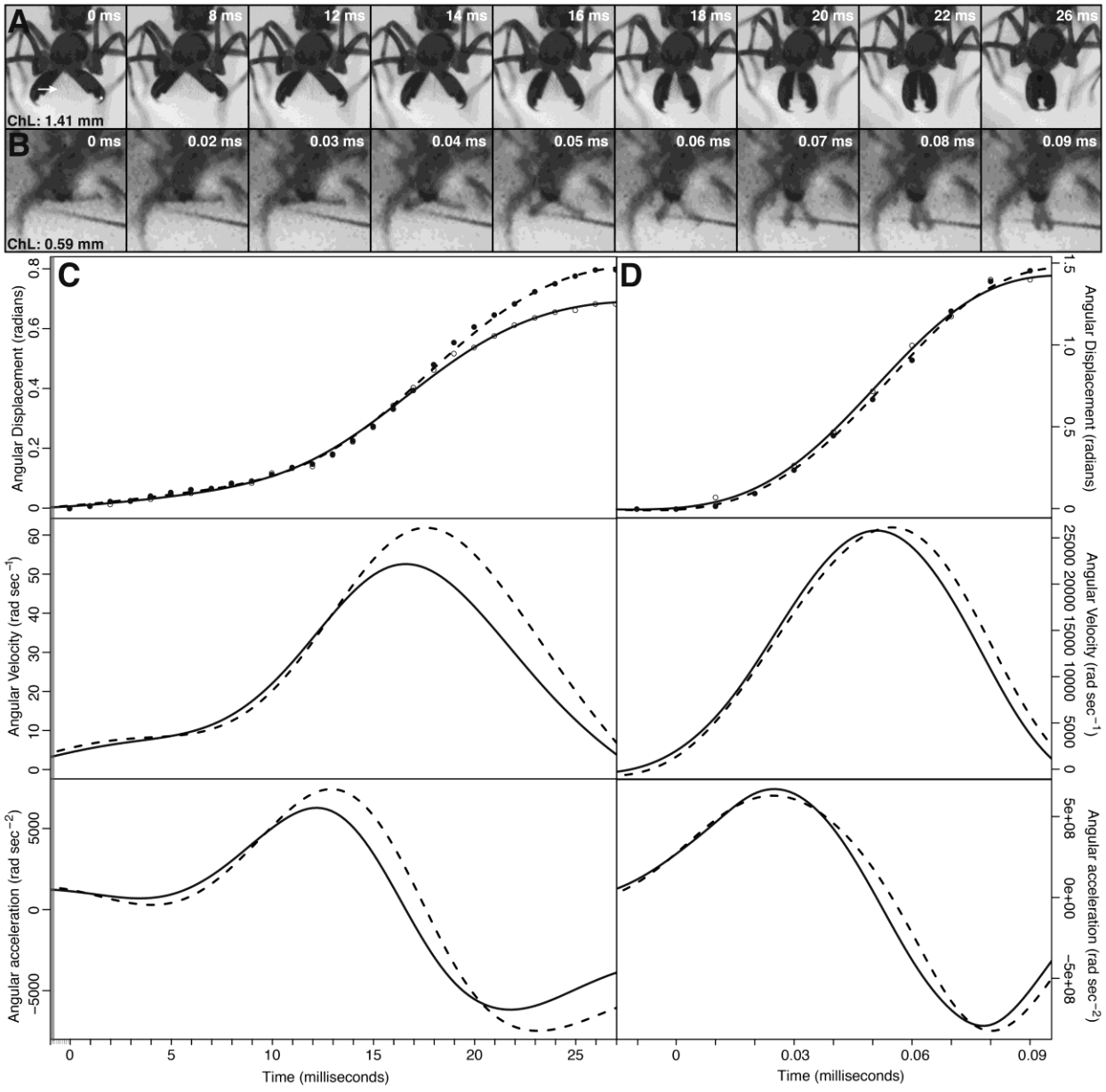

Figure 1. Kinematics and images from high-speed video recordings of *Aotearoa magna* and *Zearchaea* sp. **A.** Video frames from an *Aotearoa magna* (individual: Aotearoa2; video: C) cheliceral strike, recorded at 1,000 frames s^{-1}, with time shown in upper right corner from when chelicerae begin to move; asterisk marks the juncture between the left basal cheliceral segment

(paturon) and the fang where the movement was tracked; arrow points to a row of hairs on the left chelicera that projects anteriorly when the chelicerae are held open; ChL = average length of left and right chelicera. **B.** Video frames from a *Zearchaea* sp. (individual: ZearchVIC1; video: G) cheliceral strike, recorded at 100,000 frames s^{-1}. **C.** Kinematic data of the cheliceral strike of *Aotearoa magna* shown in (**A**). **D.** Kinematic data of the cheliceral strike of *Zearchaea* sp. shown in (**B**). **C & D.** Top panel, raw displacement data are shown for the left (solid circle) and right (open circle) chelicera, which is fitted with a spline for each chelicera (left, dashed line; right, solid line); first and second derivative of fitted spline shown in middle and bottom panel, respectively; for comparison, the grey bar in (**C**) represents 0.2 ms, and the *Zearchaea* strike in (**D**) occurs in less than half this time.

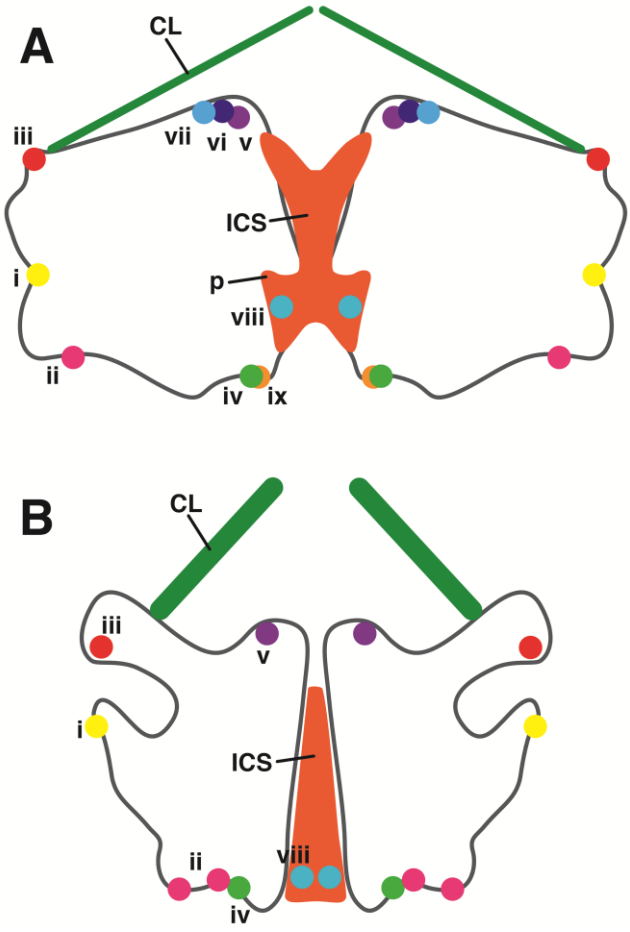

Figure 2. Illustration of cheliceral bases (**grey**) and inter-cheliceral-sclerite (ICS, **orange**), and clypeal ligaments (CL, **dark green**), dorsal view, based on μCT scans with cheliceral bases in "resting" position, showing muscle attachment sites represented as colored circles. Muscles attachment points are color-coded and labeled on the left chelicera base as in Table 1, and following Wood & Parkinson (2019): (i) **yellow**, lateral anterior; (ii) **magenta**, lateral posterior; (iii) **red**, anterior outer; (iv) **green**, posterior medial; (v) **purple**, anterior medial; (vi) **blue**, anterior medial inner; (vii) **light blue**, anterior medial outer; (viii) **aqua**, inter-cheliceral-sclerite muscle; (ix) **light orange**, endosternite muscle. **A.** *Aotearoa magna*, left projection on the inter-cheliceral-sclerite marked with a 'p'. **B.** *Zearchaea* sp.

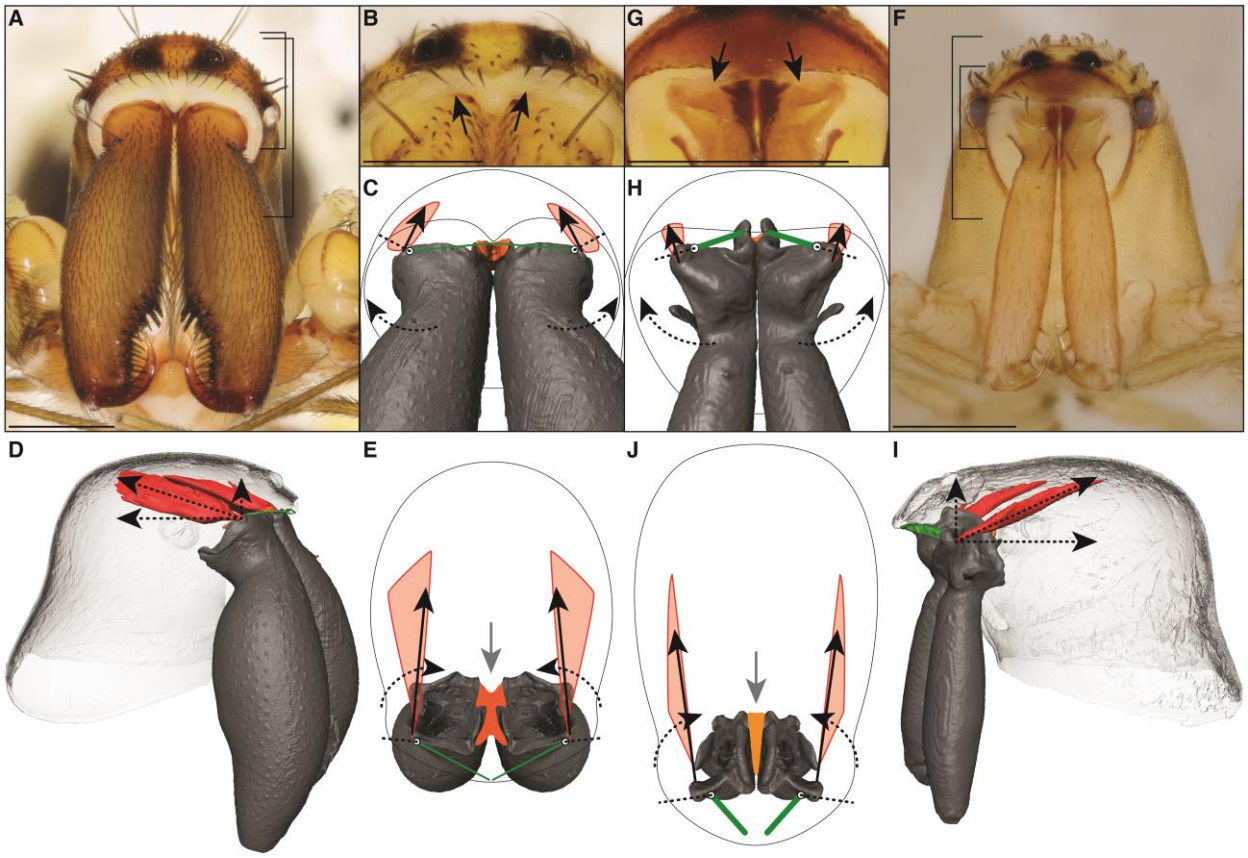

Figure 3. Morphology and musclature to open the chelicerae in *Aotearoa magna* (**A-E**) and *Zearchaea* sp. (**F-J**). **A.** Anterior view of cephalothorax in *Aotearoa* with small and large boxed sections corresponding to panel **B** and **C**, respectively, scale bar = 0.5 mm. **B.** Arrows showing clypeal ligaments in *Aotearoa*, which are barely visible as a fold in the membrane, scale bar = 0.5 mm. **F.** Anterior view of cephalothorax in *Zearchaea* with small and large boxed sections corresponding to panel **G** and **H**, respectively, scale bar = 0.25 mm. **G.** Arrows show thick clypeal ligaments in *Zearchaea* that attach the lateral anterior corner of the cheliceral bases to the pointed tip of the clypeus, scale bar = 0.25 mm. **D,I.** Different 3D surfaces segmented from μCT scans of *Aotearoa* (**D**) and *Zearchaea* (**I**), with chelicerae in the closed position, lateral-anterior view: carapace is colored translucent grey; chelicerae, **dark grey**; inter-cheliceral-sclerite, **orange**; clypeal ligaments, **dark green**; anterior outer muscles, **red**, with dashed arrows showing that the diagonal muscle force can be separated into an upward force and a backward force. **C,H.** Anterior view of cheliceral bases (**dark grey**) in resting position for *Aotearoa* (**C**) and *Zearchaea* (**H**), with the anterior outer muscles (**red**) attaching to the inside of the cheliceral

bases. Contraction of the anterior outer muscles (**red**), represented by a solid arrow, causes the chelicerae to hinge open (dashed arrow): the fulcrum occurs where clypeal ligaments (**dark green**) attach to cheliceral bases and is represented as a white circle with a black outline, and effort arms (dashed lines, length extended for visibility) are perpendicular to the line of muscle action. **E,J.** Dorsal view of cheliceral bases (**dark grey**) in resting position for *Aotearoa* (**E**) and *Zearchaea* (**J**), with the anterior outer muscles shown in **red**. Contraction of the anterior outer muscles (**red**), represented by a solid arrow, causes the chelicerae to lift and rotate outward (dashed arrow) as they open: the fulcrum is shown as a white circle with a black outline, and the effort arms (dashed lines, length extended for visibility) are perpendicular to the line of muscle action. The grey arrow represents hydraulic pressure, which may push the cheliceral bases forward in concert with contraction of the anterior outer muscles.

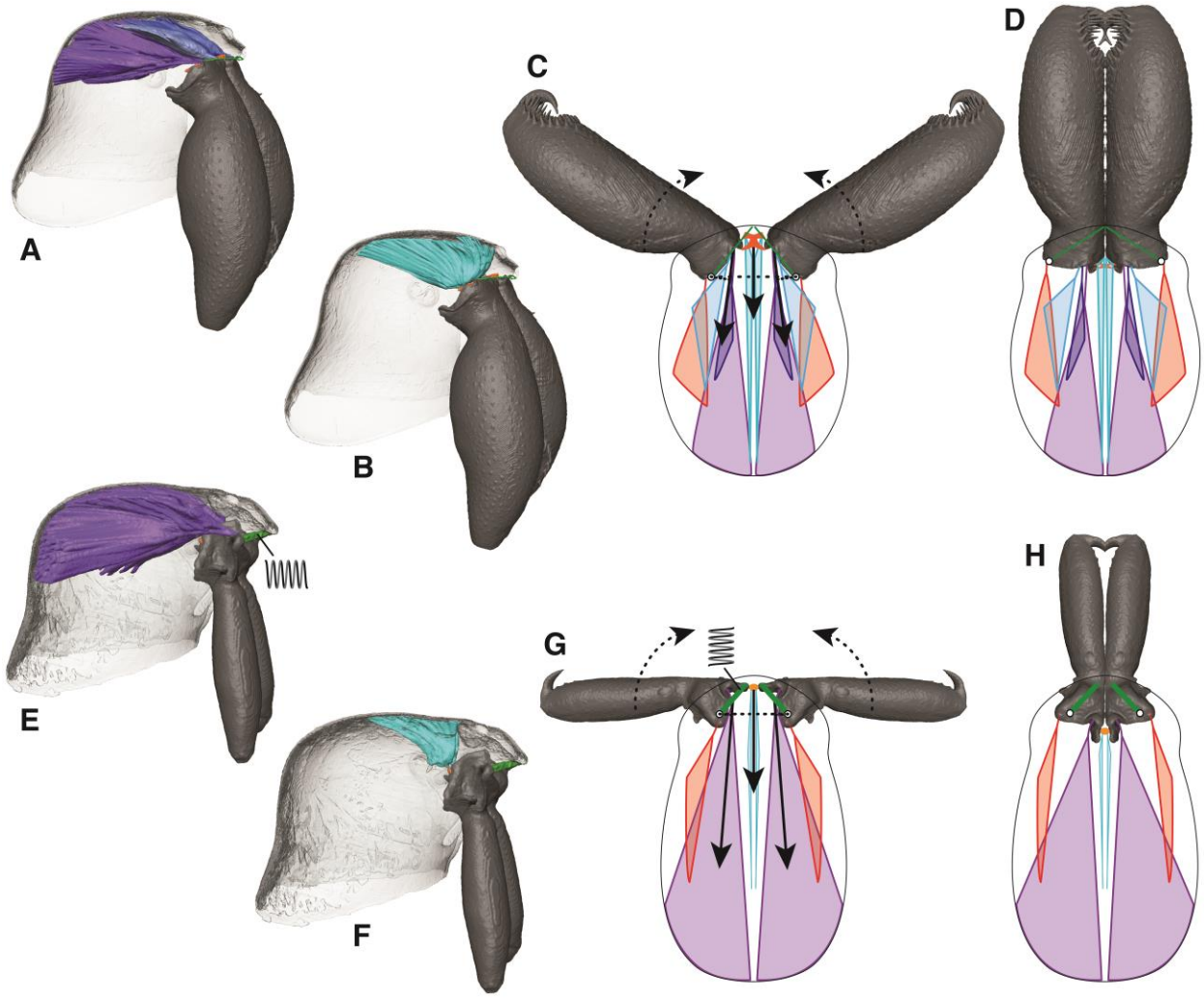

Figure 4. Musclature for cheliceral closure in *Aotearoa magna* **(A-D)** and *Zearchaea* sp. **(E-H)**. **A,B.** Different 3D surfaces segmented from a μCT scan of *Aotearoa,* with chelicerae in the closed position, lateral-anterior view: carapace is colored translucent grey; chelicerae, **dark grey**; inter-cheliceral-sclerite, **orange**; clypeal ligaments, **dark green**; anterior medial muscles, **purple**; anterior medial inner muscles, **blue**; anterior medial outer muscles, **light blue**; the inter-cheliceral-sclerite muscle (**aqua**), shown in **(B)**, runs more vertically than the other closure muscles shown in **(A)**. **E,F.** Different 3D surfaces segmented from a μCT scan of *Zearchaea,* with chelicerae in the closed position, lateral-anterior view: colors same as above, but *Zearchaea* lacks the anterior medial inner (**blue** in **A**) and the anterior medial outer (**light blue** in **A**)

muscles; the inter-cheliceral-sclerite muscles (**aqua**) shown in **(F)** runs more vertically than the other muscles; clypeal ligaments are hypothesis to stretch, represented by a spring in **(E)**, due to contraction of the anterior medial muscles (**purple**). **C,G.** Dorsal view of chelicerae (**dark grey**) in open position for *Aotearoa* **(C)** and *Zearchaea* **(G)**, based on orientation of chelicerae in high-speed videos; carapace illustrated as a line, inter-cheliceral-sclerite shown in **orange**, anterior outer abductor muscles, **red**, clypeal ligaments, **dark green**; the inter-cheliceral-sclerite muscles, **aqua**, are coming out of the page towards the viewer. In *Aotearoa* **(C)**, closure is initiated by the inter-cheliceral-sclerite muscles (**aqua**) and may be followed up by the other closure muscles (shown in **purple**, **blue**, **light blue**), represented by solid arrows, causing the chelicerae to hinge closed (dashed arrow): the fulcrum occurs where clypeal ligaments (**dark green**) attach to the cheliceral bases and is represented as a white circle with a black outline, and effort arms (dashed lines) are perpendicular to the line of muscle action. In *Zearchaea* **(G)**, the anterior medial inner and outer muscles are absent, and in the latched-open chelicerae, contraction of the anterior medial muscles (**purple**, large outer arrows) puts energy into the system by stretching the clypeal ligaments (**dark green**, represented by a spring on the left side). To close the chelicerae, the inter-cheliceral-sclerite muscles (**aqua**) contract (median arrow; effort arms shown as dashed lines), which pulls the inter-cheliceral sclerite (**orange**) backwards, releasing the stored energy in the clypeus, and the chelicerae are flung to their closed position (dashed arrow), pivoting around the fulcrum (white circle). **D,H.** The chelicerae (**dark grey**) in the closed position immediately after a strike for *Aotearoa* **(D)** and *Zearchaea* **(H)**.

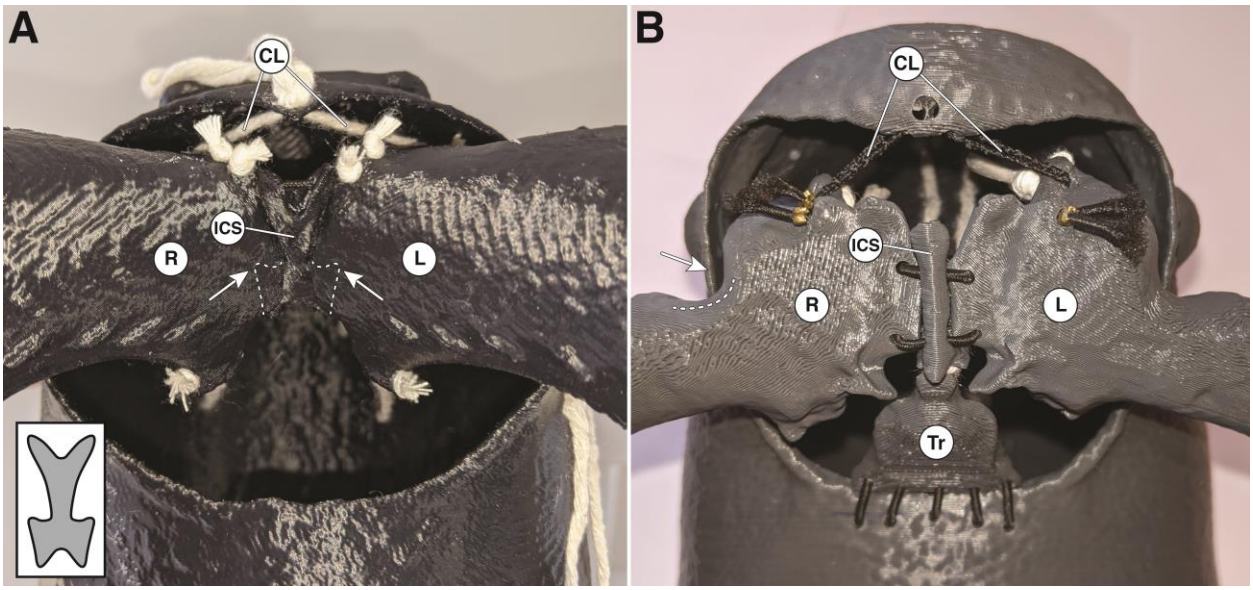

Figure 5. 3D model anterior view, with chelicerae in the open position, showing position of inter-cheliceral-sclerite (ICS) in *Aotearoa magna* (**A**) and *Zearchaea* sp. (**B**). **(A)** Position of ICS hinge showing how the ICS fits together with the cheliceral bases, 3D printed structures are black and strings are white, boxed insert shows approximate shape of ICS. In the 3D model when the chelicerae are open two projections on the ICS (approximate position shown with dashed line and white arrows) sit posterior to the cheliceral bases. The tight fit between the ICS and the cheliceral bases may serve as a hinge that guides the chelicerae open. **(B)** Hypothesized latching mechanism, 3D printed structures are grey, elastics and strings are black and white, respectively, and crimp clamps to secure the elastics are visible. In the 3D model when the chelicerae (L and R = left and right cheliceral bases) are open the inter-cheliceral-sclerite (ICS) is forward and its posterior edge has a groove that may come in contact with the top of the triangular sclerite (Tr), creating a latch. When the anterior-medial muscles (color coded purple in Figs. 2 & 4) contract the chelicerae pitch backwards, which further secures the ICS forward position and also stretches the clypeal ligaments (CL). The arrow shows the lateral edge of the carapace foramen that surrounds the cheliceral bases and may come in contact with a groove (dashed line) in the chelicerae, which may help guide the open chelicerae into position.

Supplementary Information

Figure S1

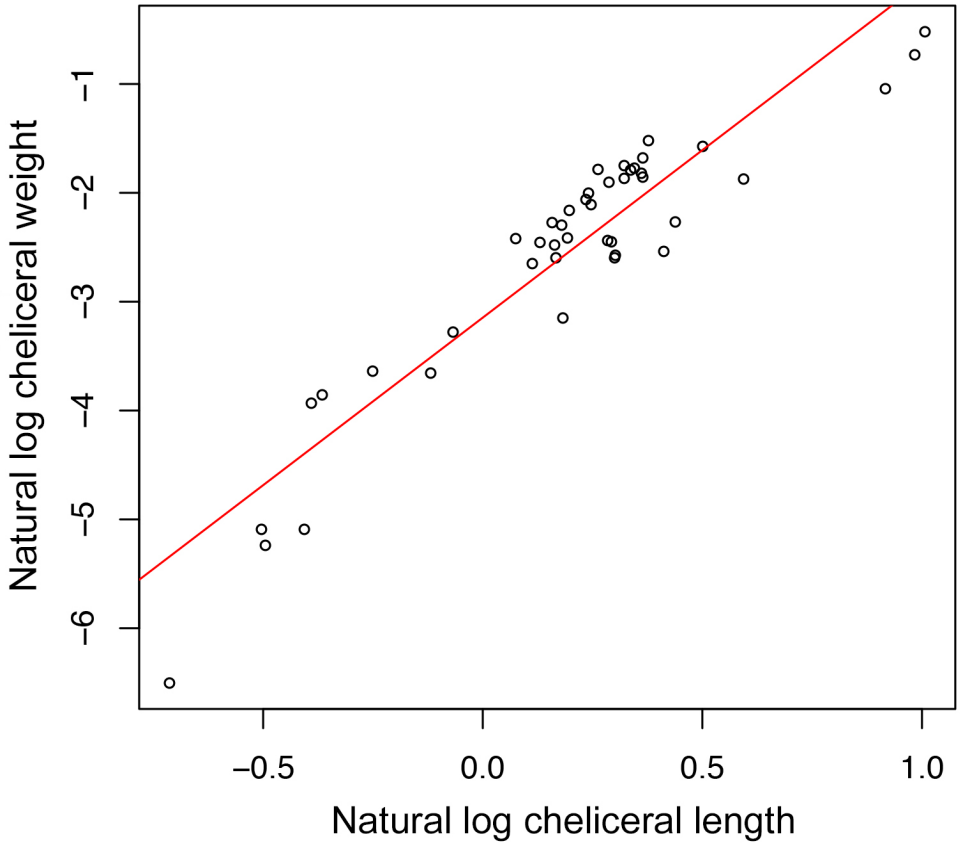

Natural log of cheliceral weight plotted against natural log of cheliceral length. A regression line was fit using the linear model command ('lm') in R (p-value < 0.001). Sample size is 43 specimens.

Figure S2

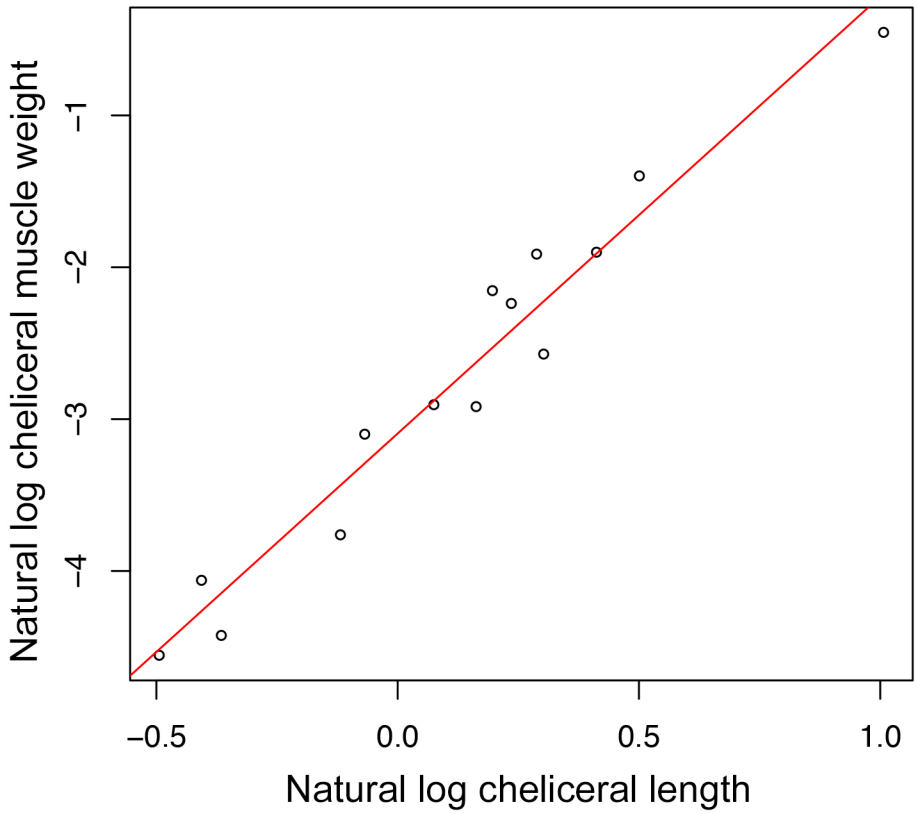

Natural log of cheliceral total muscle mass plotted against natural log of cheliceral length. A regression line was fit using the linear model command ('lm') in R (p-value < 0.001). Sample size is 14 specimens.

Figure S3

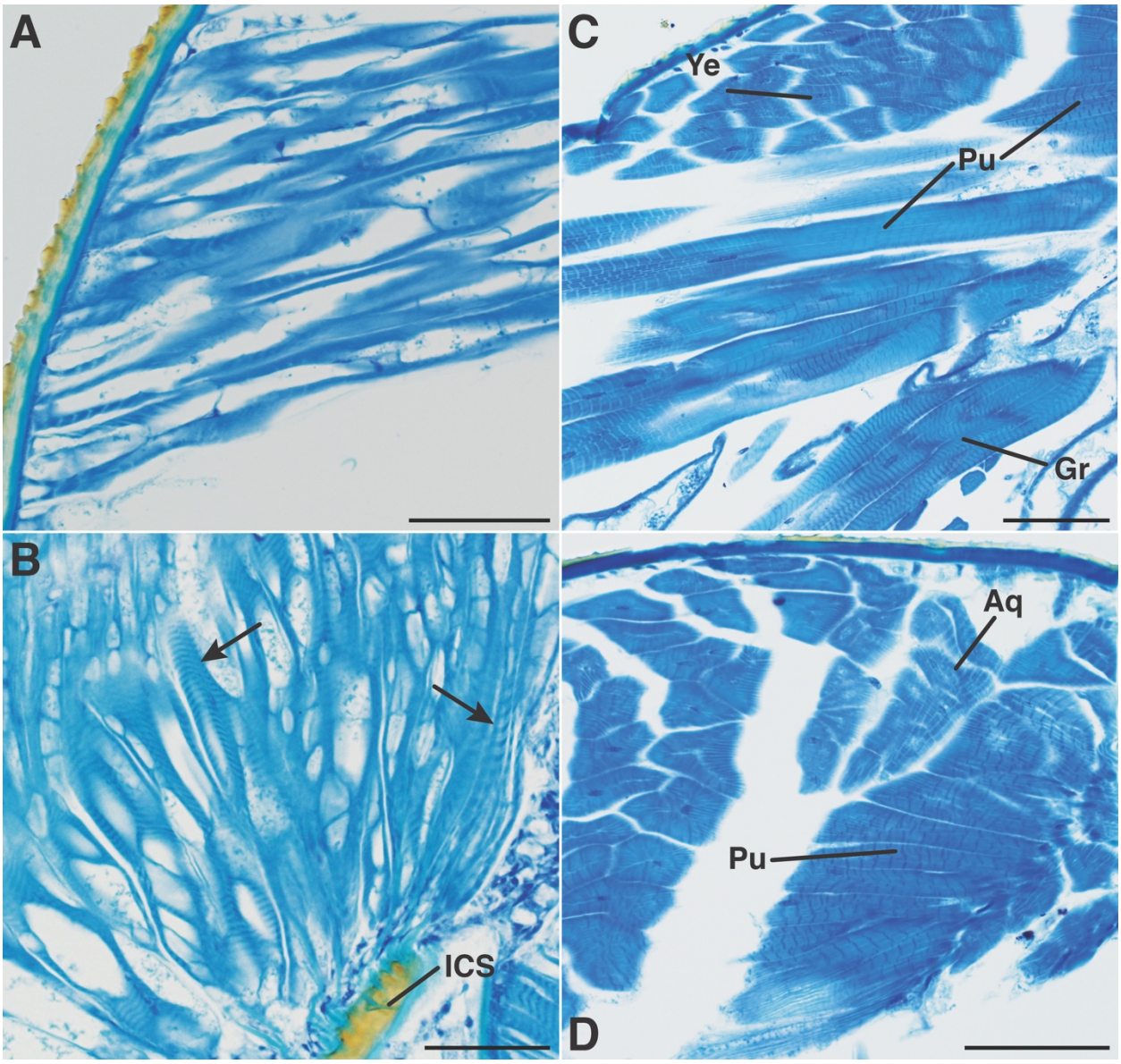

Sarcomere length differences in *Aotearoa magna* (**A-B**) and *Zearchaea* sp. (**C-D**). **A.** Anterior medial muscle (color coded purple in Figs. 2 & 4) in *Aotearoa*. **B.** Inter-cheliceral-sclerite muscle (color coded aqua in Figs. 2 & 4) in *Aotearoa*. Arrows show two different fiber types, one with shorter and one with longer sarcomeres; ICS = inter-cheliceral-sclerite. **C.** Different muscles in *Zearchaea*: Ye = lateral anterior muscle (color coded yellow in Figs. 2); Pu = anterior medial muscle (color coded purple in Figs. 2 & 4); Gr = posterior medial muscle (color coded green in Fig. 2). **D.** Different muscles in *Zearchaea*: Aq = inter-cheliceral-sclerite muscle (color coded aqua in Figs. 2 & 4); Pu = anterior medial muscle (color coded purple in Figs. 2 & 4). Scale bars = 50 μm.

Figure S4

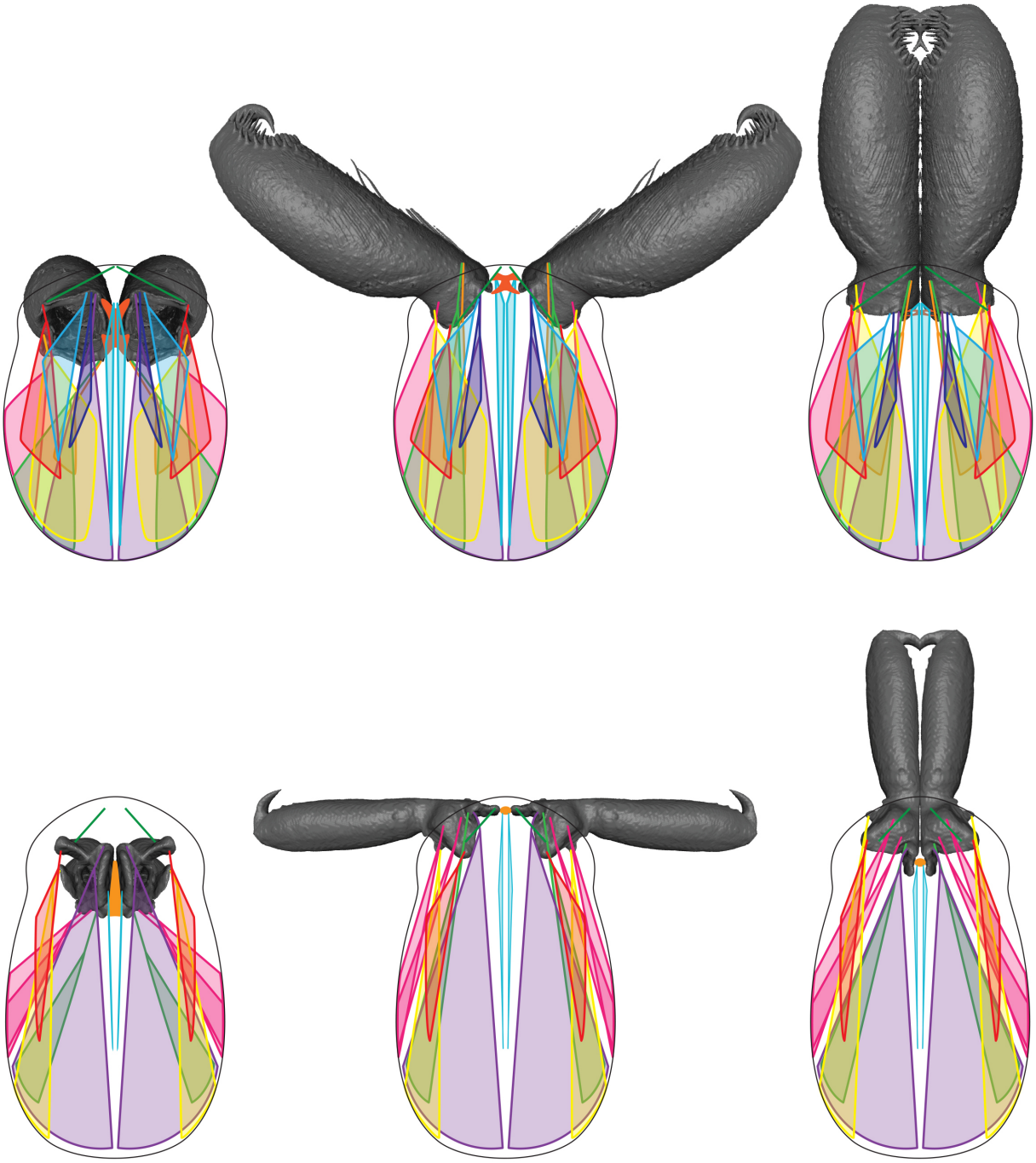

Images of all cheliceral muscles for *Aotearoa* (top) and *Zearchaea* (bottom) in the resting (left), open (middle), and closed (right) positions. The fulcrum occurs where the clypeal ligaments (green) attach to the outer lateral anterior corner of the cheliceral bases. Muscle colors follow Table 1 and Figure 2. Muscles attach to the basal edge of the chelicerae. The chelicerae are opaque dark grey and attachments were drawn on top of the chelicerae even though in many instances the muscles would connect to the posterior edge, beneath the image. For this reason, refer to Figure 2 when interpreting this image.

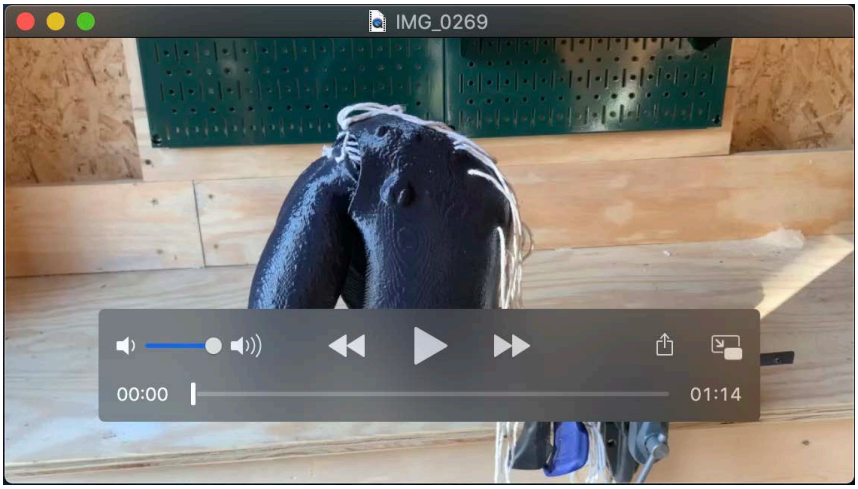

Movie 1

Movie showing operation of 3D model in *Aotearoa.*

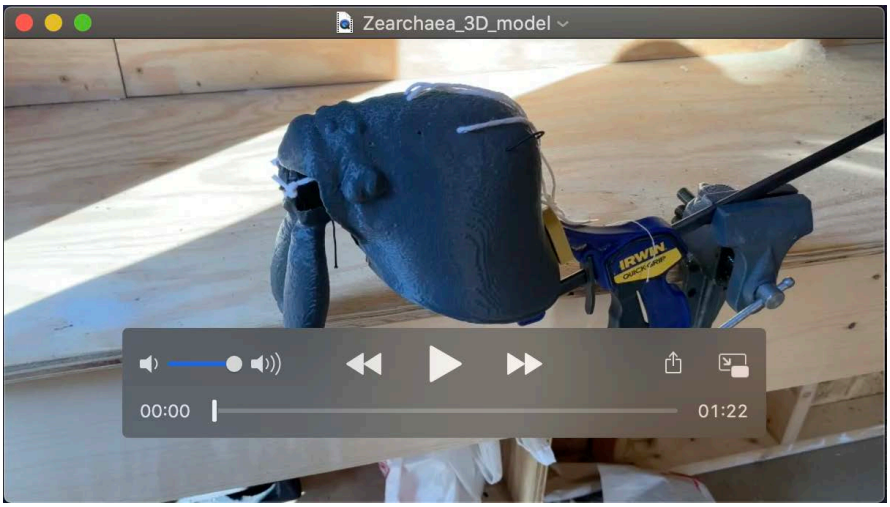

Movie 2

Movie showing operation of 3D model in *Zearchaea.*

Table S1. List of specimens used in study:

Species	Sex, museum voucher number, collection information
High-speed-videography	
Aotearoa magna	Male, museum voucher USNMENT01539031, collection information: NEW ZEALAND: Southland Region, Fiordlands National Park, Cascade Creek, near Lake Gunn outlet, Eglinton Valley, ~64 km NE Te Anau, elev. 500m, S44°53.683' E168°04.918', 13 Mar 2018, sifting moss on tree trunk bases and fallen logs in *Nothofagus* forest, H. Wood, code: HW0109A
Aotearoa magna	Male, museum voucher USNMENT01539032, collection information: NEW ZEALAND: Southland Region, Fiordlands National Park, Cascade Creek, near Lake Gunn outlet, Eglinton Valley, ~64 km NE Te Anau, elev. 500m, S44°53.683' E168°04.918', 13 Mar 2018, sifting moss on tree trunk bases and fallen logs in *Nothofagus* forest, H. Wood, code: HW0109A
Zearchaea morphospecies 1	Penultimate female, museum voucher USNMENT01539033, collection information: NEW ZEALAND: West Coast region, Victoria Conservation Park,down Capelston Rd., beginning of Kirwan's Track, S42º04'00.4", E171º55'24.1", elev. 210 m, sifting litter in disturbed *Nothofagus* forest, Nov 18-19, 2018, H. Wood & T. Nguyen, code: HW0120C
Zearchaea morphospecies 2	Female, museum voucher USNMENT01539030, collection information: NEW ZEALAND: Canterbury Region, close to Lewis Pass, on the southern entrance to St. James Walkway, ~35.8 km W of Hanmer Springs, S42°31'09.7"E172°23'37.4", elev 620m, 18-24 Mar 2011, sifting dense moss on trees, ground, and around logs in daytime in native *Nothofagus* forest, H. Wood, code: HW0075
Zearchaea morphospecies 2	Female, museum voucher USNMENT01377164, collection information: NEW ZEALAND: Canterbury Region, Lewis Pass, hiked in ~1 km from the northern entrance of St. James Walkway, ~18.7 km E of Springs Junction, S42° 22' 43.0"E172° 24' 06.3", elev 860m, 20-23 Mar 2011, sifting litter and moss on trees, ground, and around logs in daytime in native *Nothofagus* forest, H. Wood, code: HW0076
Histology specimens	
Aotearoa magna	Male, museum voucher USNMENT01539034, collection information: NEW ZEALAND: Southland Region, Fiordlands National Park, Cascade Creek, near Lake Gunn outlet, Eglinton Valley, ~64 km NE Te Anau, elev. 500m, S44°53.683' E168°04.918', 13 Mar 2018, sifting moss on tree trunk bases and fallen logs in *Nothofagus* forest, H. Wood, code: HW0109A
Zearchaea morphospecies 3	Female, museum voucher: USNMENT01458827, collection information: NEW ZEALAND: Canterbury Region, near Arthur's Pass, Woolshed Hill track,≈5.5 km N of Cass UC Field Station, elev. 600m - 900m, 18 July 2008, S42°59'12.1" E171°45'12.3", sifting litter and moss on trees, ground, and around logs in daytime, sifting close to stream and higher up in elevation away from stream in *Nothofagus* forest, H. Wood,code: HW110
µ-Computed tomography scans (Wood & Parkinson, 2019)	
Aotearoa magna	Female, museum voucher CASENT9028269, collection information: NEW ZEALAND: South Island, Fiordland, Gunn's Camp, Feb. 1986, R. Forster *Zearchaea* morphospecies 2, female, museum voucher USNMENT01377164, collection information: NEW ZEALAND: Canterbury Region, Lewis Pass, hiked in ~1 km from the northern entrance of St. James Walkway, ~18.7 km E of Springs Junction, S42° 22' 43.0"E172° 24' 06.3", elev 860m, 20-23 Mar 2011, sifting litter and moss on trees, ground, and around logs in daytime in native
	Nothofagus forest, H. Wood, code: HW0076

USNMENT, US National Museum, Department of Entomology; CASENT = California Academy of Sciences, Department of Entomology.

Supplementary Information

Figure S1

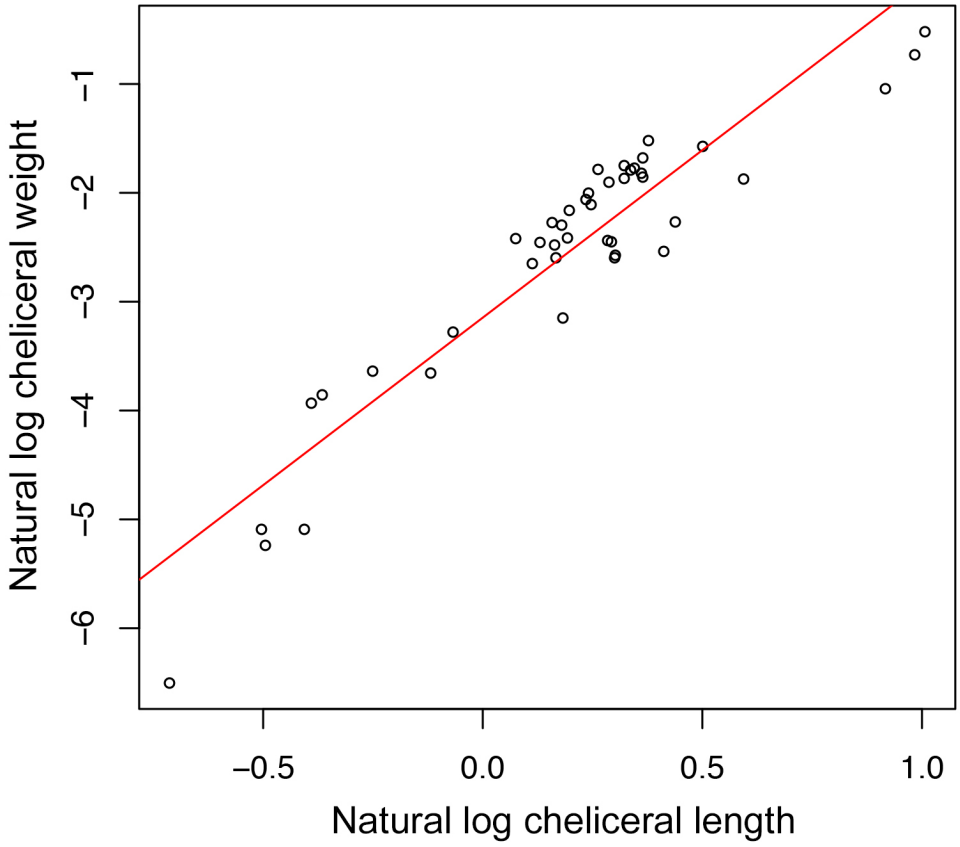

Natural log of cheliceral weight plotted against natural log of cheliceral length. A regression line was fit using the linear model command ('lm') in R (p-value < 0.001). Sample size is 43 specimens.

Figure S2

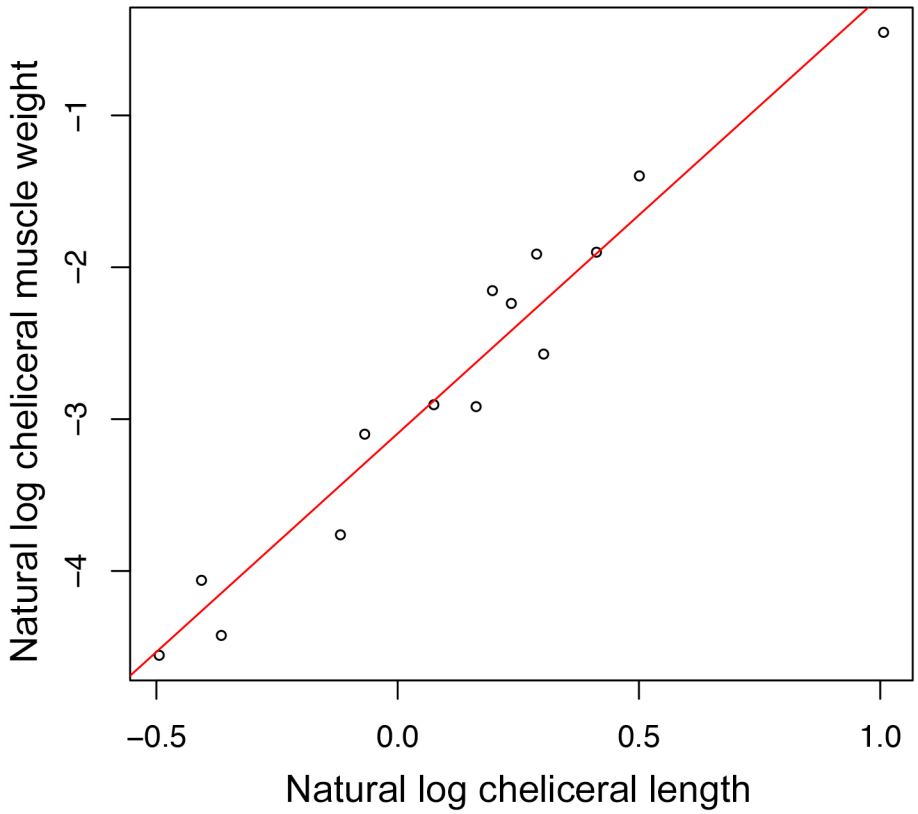

Natural log of cheliceral total muscle mass plotted against natural log of cheliceral length. A regression line was fit using the linear model command ('lm') in R (p-value < 0.001). Sample size is 14 specimens.

Figure S3

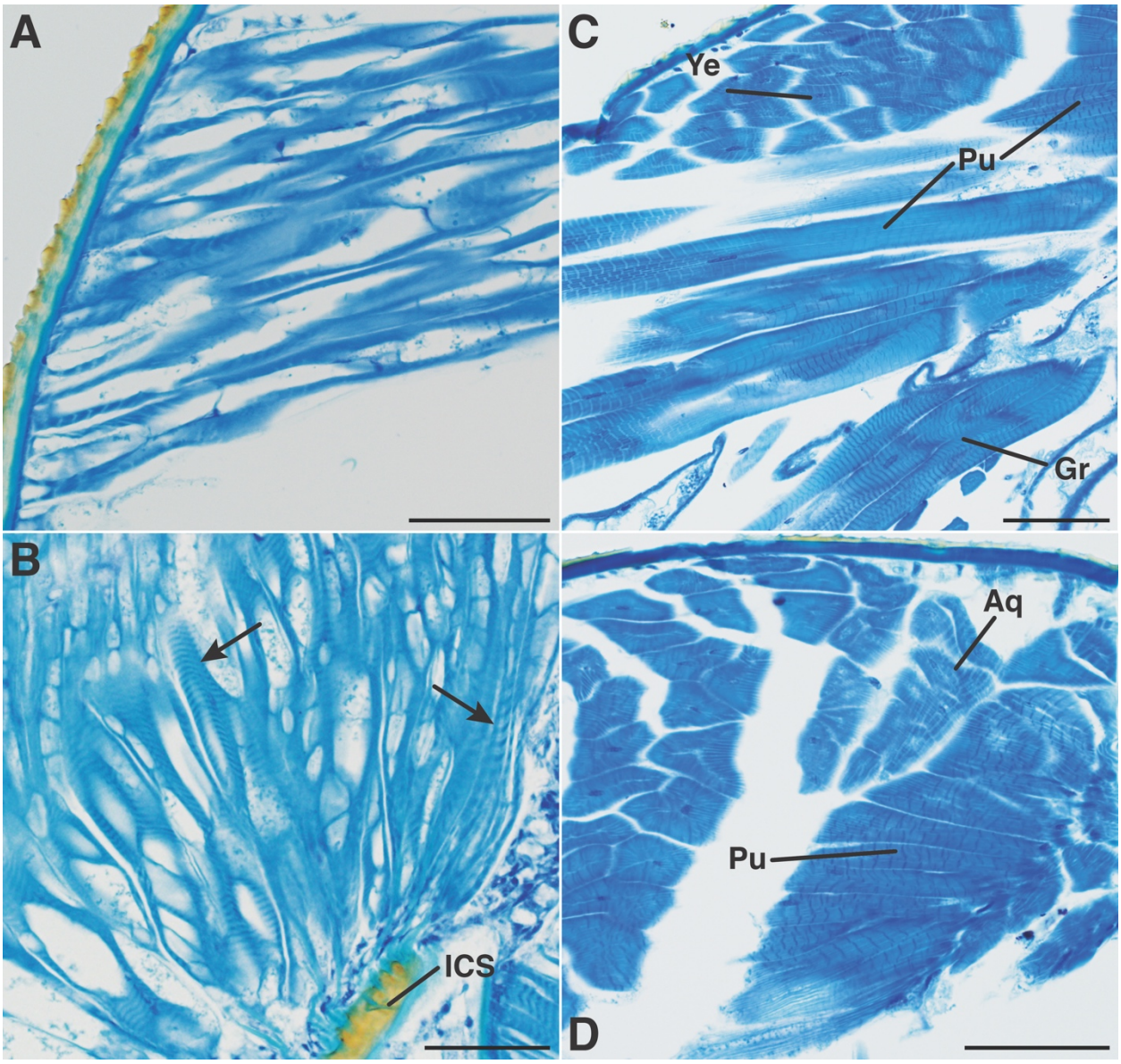

Sarcomere length differences in *Aotearoa magna* (**A-B**) and *Zearchaea* sp. (**C-D**). **A.** Anterior medial muscle (color coded purple in Figs. 2 & 4) in *Aotearoa*. **B.** Inter-cheliceral-sclerite muscle (color coded aqua in Figs. 2 & 4) in *Aotearoa*. Arrows show two different fiber types, one with shorter and one with longer sarcomeres; ICS = inter-cheliceral-sclerite. **C.** Different muscles in *Zearchaea*: Ye = lateral anterior muscle (color coded yellow in Figs. 2); Pu = anterior medial muscle (color coded purple in Figs. 2 & 4); Gr = posterior medial muscle (color coded green in Fig. 2). **D.** Different muscles in *Zearchaea*: Aq = inter-cheliceral-sclerite muscle (color coded aqua in Figs. 2 & 4); Pu = anterior medial muscle (color coded purple in Figs. 2 & 4). Scale bars = 50 μm.

Figure S4

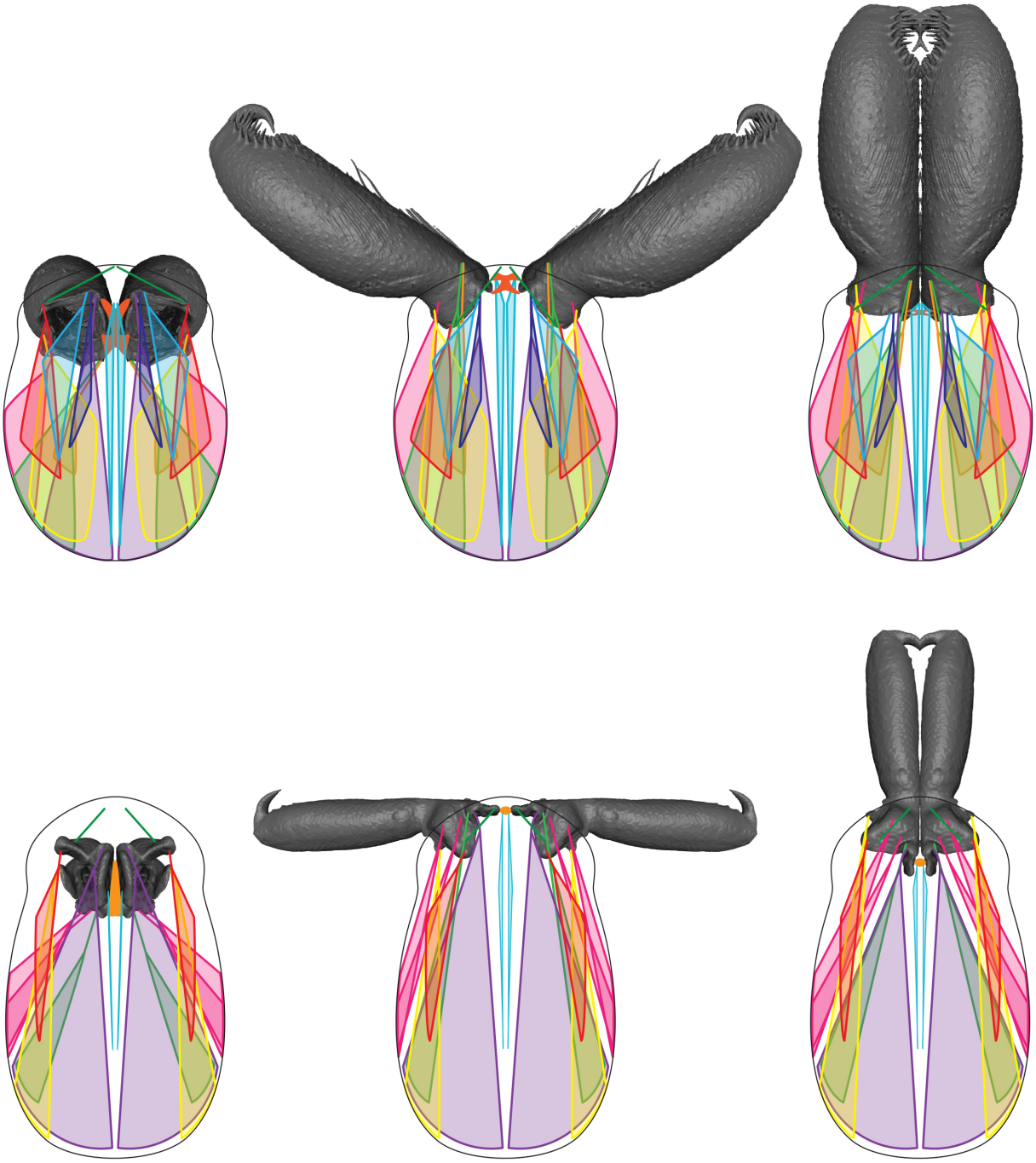

Images of all cheliceral muscles for *Aotearoa* (top) and *Zearchaea* (bottom) in the resting (left), open (middle), and closed (right) positions. The fulcrum occurs where the clypeal ligaments (green) attach to the outer lateral anterior corner of the cheliceral bases. Muscle colors follow Table 1 and Figure 2. Muscles attach to the basal edge of the chelicerae. The chelicerae are opaque dark grey and attachments were drawn on top of the chelicerae even though in many instances the muscles would connect to the posterior edge, beneath the image. For this reason, refer to Figure 2 when interpreting this image.

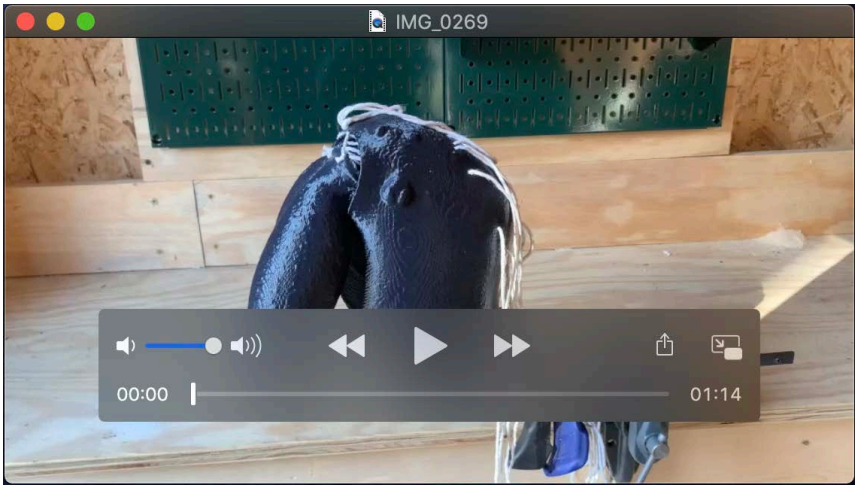

Movie 1

Movie showing operation of 3D model in *Aotearoa.*

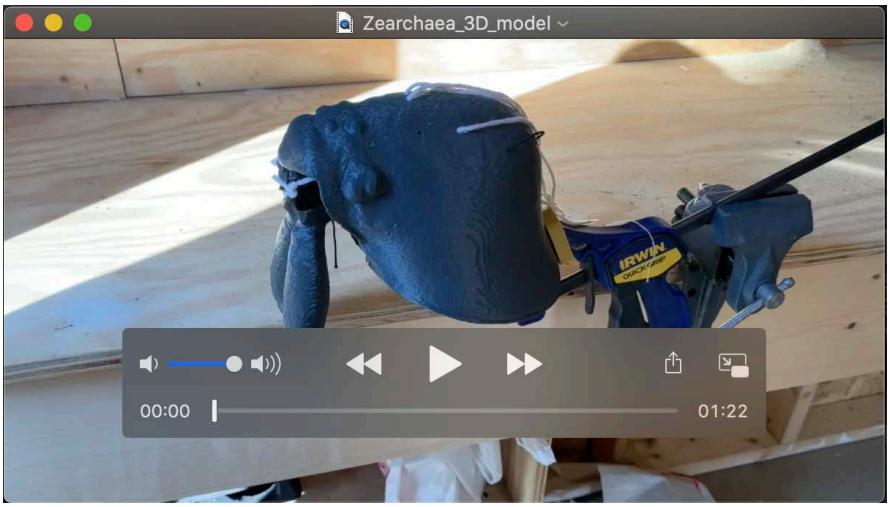

Movie 2

Movie showing operation of 3D model in *Zearchaea.*

Table S1. List of specimens used in study

Species	Sex, museum voucher number, collection information
High-speed-videography	
Aotearoa magna	Male, museum voucher USNMENT01539031, collection information: NEW ZEALAND: Southland Region, Fiordlands National Park, Cascade Creek, near Lake Gunn outlet, Eglinton Valley, ~64 km NE Te Anau, elev. 500m, S44°53.683' E168°04.918', 13 Mar 2018, sifting moss on tree trunk bases and fallen logs in *Nothofagus* forest, H. Wood, code: HW0109A
Aotearoa magna	Male, museum voucher USNMENT01539032, collection information: NEW ZEALAND: Southland Region, Fiordlands National Park, Cascade Creek, near Lake Gunn outlet, Eglinton Valley, ~64 km NE Te Anau, elev. 500m, S44°53.683' E168°04.918', 13 Mar 2018, sifting moss on tree trunk bases and fallen logs in *Nothofagus* forest, H. Wood, code: HW0109A
Zearchaea morphospecies 1	Penultimate female, museum voucher USNMENT01539033, collection information: NEW ZEALAND: West Coast region, Victoria Conservation Park,down Capelston Rd., beginning of Kirwan's Track, S42º04'00.4", E171º55'24.1", elev. 210 m, sifting litter in disturbed *Nothofagus* forest, Nov 18-19, 2018, H. Wood & T. Nguyen, code: HW0120C
Zearchaea morphospecies 2	Female, museum voucher USNMENT01539030, collection information: NEW ZEALAND: Canterbury Region, close to Lewis Pass, on the southern entrance to St. James Walkway, ~35.8 km W of Hanmer Springs, S42°31'09.7"E172°23'37.4", elev 620m, 18-24 Mar 2011, sifting dense moss on trees, ground, and around logs in daytime in native *Nothofagus* forest, H. Wood, code: HW0075
Zearchaea morphospecies 2	Female, museum voucher USNMENT01377164, collection information: NEW ZEALAND: Canterbury Region, Lewis Pass, hiked in ~1 km from the northern entrance of St. James Walkway, ~18.7 km E of Springs Junction, S42° 22' 43.0"E172° 24' 06.3", elev 860m, 20-23 Mar 2011, sifting litter and moss on trees, ground, and around logs in daytime in native *Nothofagus* forest, H. Wood, code: HW0076
Histology specimens	
Aotearoa magna	Male, museum voucher USNMENT01539034, collection information: NEW ZEALAND: Southland Region, Fiordlands National Park, Cascade Creek, near Lake Gunn outlet, Eglinton Valley, ~64 km NE Te Anau, elev. 500m, S44°53.683' E168°04.918', 13 Mar 2018, sifting moss on tree trunk bases and fallen logs in *Nothofagus* forest, H. Wood, code: HW0109A
Zearchaea morphospecies 3	Female, museum voucher: USNMENT01458827, collection information: NEW ZEALAND: Canterbury Region, near Arthur's Pass, Woolshed Hill track,≈5.5 km N of Cass UC Field Station, elev. 600m - 900m, 18 July 2008, S42°59'12.1" E171°45'12.3", sifting litter and moss on trees, ground, and around logs in daytime, sifting close to stream and higher up in elevation away from stream in *Nothofagus* forest, H. Wood,code: HW110
µ-Computed tomography scans (Wood & Parkinson, 2019)	
Aotearoa magna	Female, museum voucher CASENT9028269, collection information: NEW ZEALAND: South Island, Fiordland, Gunn's Camp, Feb. 1986, R. Forster
Zearchaea morphospecies 2	Female, museum voucher USNMENT01377164, collection information: NEW ZEALAND: Canterbury Region, Lewis Pass, hiked in ~1 km from the northern entrance of St. James Walkway, ~18.7 km E of Springs Junction, S42° 22' 43.0"E172° 24' 06.3", elev 860m, 20-23 Mar 2011, sifting litter and moss on trees, ground, and around logs in daytime in native *Nothofagus* forest, H. Wood, code: HW0076

USNMENT, US National Museum, Department of Entomology; CASENT = California Academy of Sciences, Department of Entomology.